

IMPACTS OF FLY ASH COMPOSITION AND FLUE GAS COPONENTS ON  
MERCURY SPECIATION

by

Xihua Chen

B. S., Environmental Science, University of Science of Technology of China, 2004

Submitted to the Graduate Faculty of

The School of Engineering in partial fulfillment

of the requirements for the degree of

Master of Science

University of Pittsburgh

2007

UNIVERSITY OF PITTSBURGH  
SCHOOL OF ENGINEERING

This thesis was presented

by

Xihua Chen

It was defended on

July 9, 2007

and approved by

Radisav D. Vidić, Professor, Department of Civil and Environmental Engineering

Götz Vesper, Assistant Professor, Department of Chemical and Petroleum Engineering

Jason D. Monnell, Visiting Assistant Professor, Department of Civil and Environmental  
Engineering

Thesis Advisor: Radisav D. Vidić, Professor, Department of Civil and Environmental  
Engineering

## IMPACTS OF FLY ASH COMPOSITION AND FLUE GAS COPONENTS ON MERCURY SPECIATION

Xihua Chen, M.S.

University of Pittsburgh, 2007

The impact of six fly ash samples on mercury speciation in simulated flue gas was evaluated in this study. A fixed bed reactor system was used to study the catalytic effect of fly ash on mercury oxidation at temperature of 140 °C in simulated flue gas consisting of N<sub>2</sub>, CO<sub>2</sub>, O<sub>2</sub>, NO, NO<sub>2</sub>, SO<sub>2</sub>, HCl, and H<sub>2</sub>O. Mercury was introduced to the reactor using a temperature controlled permeation tube. Elemental and total mercury in the effluent were measured using a semi-continuous atomic fluorescence mercury monitor. Fly ash samples were characterized using SEM-EDAX, XRD, TGA, BET analyzer and particle size analyzer. Mercury uptake tests with different fly ash samples revealed that LOI (Loss On Ignition), surface area, and particle size all had positive effects on mercury oxidation and adsorption.

Experiments with pure components showed that alumina (Al<sub>2</sub>O<sub>3</sub>), silica (SiO<sub>2</sub>), calcium oxide (CaO), magnesium oxide (MgO), and titania (TiO<sub>2</sub>) did not promote mercury oxidation or capture. Ferric oxide (Fe<sub>2</sub>O<sub>3</sub>), and unburned carbon were found to have profound effects on mercury oxidation and capture. Unburned carbon is considered the most important fly ash component for mercury oxidation due to much larger presence in fly ash than Fe<sub>2</sub>O<sub>3</sub>.

Experiments with carbon black and different flue gas composition revealed the importance of the interaction between flue gas and surface on mercury uptake. Oxygen containing surface functionalities did not enhance adsorption or oxidation of mercury by themselves.  $\text{NO}_2$  and  $\text{HCl}$  promoted mercury oxidation and adsorption on carbon black. Addition of  $\text{O}_2$  to  $\text{HCl}$  containing gas stream significantly improved mercury adsorption and oxidation.  $\text{SO}_2$  seems to inhibit both mercury oxidation and adsorption.  $\text{NO}$  and  $\text{H}_2\text{O}$  had little impact on mercury oxidation or adsorption in inert gas flow.  $\text{H}_2\text{O}$  may inhibit mercury adsorption in early stages of the experiment, but the inhibitory effect diminished over time.

**Keywords:** Mercury (Hg), Fly Ash, Flue Gas, Speciation, Oxidation, Adsorption

## TABLE OF CONTENTS

|   |           |
|---|-----------|
| <b>ACKNOWLEDGEMENTS .....</b>                                   | <b>XI</b> |
| <b>1.0 INTRODUCTION.....</b>                                    | <b>1</b>  |
| <b>2.0 LITERATURE REVIEW .....</b>                              | <b>3</b>  |
| <b>2.1 MERCURY TRANSFORMATION IN GAS PHASE.....</b>             | <b>3</b>  |
| <b>2.2 MERCURY TRANSFORMATION IN HETEROGENEOUS SYSTEMS.....</b> | <b>8</b>  |
| <b>2.2.1 Coal Composition .....</b>                             | <b>9</b>  |
| <b>2.2.2 Impact of Fly Ash .....</b>                            | <b>11</b> |
| <b>2.2.3 Impact of Flue Gas Components.....</b>                 | <b>14</b> |
| <b>2.2.3.1 Hydrogen Chloride (HCl) .....</b>                    | <b>15</b> |
| <b>2.2.3.2 Sulfur Dioxide (SO<sub>2</sub>) .....</b>            | <b>16</b> |
| <b>2.2.3.3 Nitrogen Oxides (NO<sub>x</sub>) .....</b>           | <b>17</b> |
| <b>2.2.3.4 Water Vapor (H<sub>2</sub>O) .....</b>               | <b>20</b> |
| <b>2.3 SUMMARY AND RESEARCH NEEDS .....</b>                     | <b>20</b> |
| <b>3.0 MATERIALS AND METHODS .....</b>                          | <b>21</b> |
| <b>3.1 SAMPLES.....</b>   | <b>21</b> |
| <b>3.2 EXPERIMENT SETUP AND PROCEDURE.....</b>                  | <b>22</b> |
| <b>3.3 FLY ASH CHARACTERIZATION .....</b>                       | <b>25</b> |
| <b>3.3.1 Surface Area Analysis .....</b>                        | <b>25</b> |

|       |   |    |
|-------|---|----|
| 3.3.2 | Particle Size Distribution Analysis .....   | 25 |
| 3.3.3 | SEM-EDAX Analysis .....   | 25 |
| 3.3.4 | X-ray Diffraction Analysis.....   | 26 |
| 3.3.5 | X-ray Photoelectron Spectroscopy (XPS) Analysis.....                                    | 26 |
| 3.3.6 | Loss On Ignition (LOI) and Moisture Analysis.....                                       | 26 |
| 3.3.7 | TPD Analysis.....   | 27 |
| 4.0   | RESULTS AND DISCUSSION .....  | 29 |
| 4.1   | FLY ASH CHARACTERIZATION .....  | 29 |
| 4.1.1 | Surface Area Analysis .....   | 29 |
| 4.1.2 | LOI and Moisture Analysis .....   | 29 |
| 4.1.3 | SEM Graphs .....  | 31 |
| 4.1.4 | Particle Size Distribution.....   | 32 |
| 4.1.5 | Surface Chemical Properties.....  | 33 |
| 4.2   | MERCURY UPTAKE TESTS.....   | 35 |
| 4.2.1 | Baseline.....   | 35 |
| 4.2.2 | Mercury Speciation Tests with Fly ash samples.....                                      | 37 |
| 4.2.3 | Mercury Speciation Tests with Synthetic Single Components....                           | 44 |
| 4.2.4 | Mercury Speciation Tests with Carbon Black under Different<br>Flue Gas Composition..... | 52 |
| 5.0   | SUMMARY AND CONCLUSIONS .....   | 68 |
|       | BIBLIOGRAPHY.....   | 70 |

## LIST OF TABLES

|  |    |
|--|----|
| Table 1 General Characteristics of Power Plants.....   | 21 |
| Table 2 Composition of Simulated Flue Gas.....   | 23 |
| Table 3 Surface Area Analysis Results.....   | 29 |
| Table 4 LOI and Moisture Analysis.....   | 30 |
| Table 5 Mean Particle Sizes.....   | 33 |
| Table 6 Surface Elemental Composition from EDAX Analysis on fly Ash Samples .....  | 33 |
| Table 7 Surface Elemental Composition (Atom Ratio) from XPS Analysis.....  | 34 |
| Table 8 Surface Elemental Composition (Weight Ratio) from XPS Analysis .....   | 34 |
| Table 9 Hg uptake and oxidation after four-hour exposure with fly ash.....   | 41 |
| Table 10 Hg Uptake and Oxidation after Four-hour Exposure with Fly .....   | 51 |
| Table 11 TPD and XPS Analyses of Carbon Black Samples Treated with Different Flue Gas Combination.....                   | 52 |
| Table 12 Hg Uptake and Oxidation after Four-hour Exposure with SH Fly Ash in Flue Gas with and without Water Vapor ..... | 59 |

## LIST OF FIGURES

|  |    |
|--|----|
| Figure 1. Equilibrium distribution of elemental and oxidized mercury from various HCl concentrations <sup>5</sup> .....  | 4  |
| Figure 2. Percentage of mercury as (A) gas-phase elemental and (B) particulate bound at the inlet of particulate control devices based on ICR data. ESP= Electrostatic Precipitator, FF= Fabric Filter, and HESP=hot-side ESP. Trend lines taken from the ICR data were not statistically determined. <sup>4</sup> ..... | 10 |
| Figure 3. Suggested heterogeneous model for mercury capture showing potential impact of acid gases <sup>4</sup> .....  | 19 |
| Figure 4. Schematic of the Hg uptake test setup.....   | 22 |
| Figure 5. 200X SEM graphs of fly ash sample a) SH, b) Brayton, c) Gaston, d) PP, e) CE1 and f) CE2.....  | 31 |
| Figure 6. Size distribution of Brayton Point fly ash sample.....   | 32 |
| Figure 7. A typical baseline run with flue gas at 140 °C .....   | 35 |
| Figure 8. A 10-hr baseline run with flue gas at 140°C .....  | 36 |
| Figure 9. Hg uptake test with 50 mg CE1 fly ash at 140 °C.....   | 37 |
| Figure 10. Hg uptake test with 50 mg CE2 fly ash at 140 °C.....  | 38 |
| Figure 11. Hg uptake test with 50 mg PP fly ash at 140 °C.....   | 39 |
| Figure 12. Hg uptake test with 50 mg Gaston fly ash at 140 °C.....   | 39 |
| Figure 13. Hg uptake test with 50 mg Brayton fly ash at 140 °C .....   | 40 |
| Figure 14. Hg uptake test with 50 mg SH fly ash at 140 °C.....   | 40 |
| Figure 15. Effects of surface area on Hg uptake and oxidation at 140 °C.....   | 42 |



|  |    |
|--|----|
| Figure 16. Effects of particle size on Hg uptake and oxidation at 140 °C.....  | 43 |
| Figure 17. Effects of LOI% on Hg uptake and oxidation at 140 °C.....   | 44 |
| Figure 18. Hg uptake test with 8 g raw sand at 140 °C.....   | 45 |
| Figure 19. Hg uptake test with 4 g treated sand at 140 °C.....   | 45 |
| Figure 20. Hg uptake test with 50 mg CaO at 140 °C.....  | 46 |
| Figure 21. Hg uptake test with 50 mg MgO at 140 °C .....   | 47 |
| Figure 22. Hg uptake test with 50 mg Al <sub>2</sub> O <sub>3</sub> at 140 °C .....  | 47 |
| Figure 23. Hg uptake test with 50 mg TiO <sub>2</sub> at 140 °C .....  | 48 |
| Figure 24. Hg uptake test with 50 mg Fe <sub>2</sub> O <sub>3</sub> at 140 °C .....  | 49 |
| Figure 25. Hg uptake test with 50 mg carbon black at 140 °C .....  | 50 |
| Figure 26 Hg uptake by carbon black in N <sub>2</sub> at 140 °C .....  | 53 |
| Figure 27. Hg uptake by carbon black in N <sub>2</sub> + CO <sub>2</sub> + O <sub>2</sub> at 140 °C.....                               | 54 |
| Figure 28. TPD analysis of as-received carbon black.....   | 54 |
| Figure 29. Effects of SO <sub>2</sub> on Hg uptake by carbon black in N <sub>2</sub> at 140 °C .....                                   | 55 |
| Figure 30. Effects of SO <sub>2</sub> on Hg uptake by carbon black in N <sub>2</sub> + CO <sub>2</sub> + O <sub>2</sub> at 140 °C....  | 55 |
| Figure 31. Effects of NO on Hg uptake by carbon black at 140 °C .....  | 56 |
| Figure 32 Effects of H <sub>2</sub> O on Hg uptake by carbon black in N <sub>2</sub> + CO <sub>2</sub> + O <sub>2</sub> at 140 °C .... | 57 |
| Figure 33. Effects of H <sub>2</sub> O on Hg uptake by SH fly ash in flue gas at 140 °C .....  | 58 |
| Figure 34. Effects of NO <sub>2</sub> on Hg uptake by carbon black in N <sub>2</sub> at 140 °C.....                                    | 59 |
| Figure 35. Effects of NO <sub>2</sub> on Hg uptake by carbon black in N <sub>2</sub> + CO <sub>2</sub> + O <sub>2</sub> at 140 °C ...  | 60 |
| Figure 36. Effects of HCl on Hg uptake by carbon black in N <sub>2</sub> at 140 °C .....   | 61 |
| Figure 37. Effects of HCl on Hg uptake by carbon black in N <sub>2</sub> +CO <sub>2</sub> +O <sub>2</sub> at 140 °C.....               | 63 |

|   |    |
|---|----|
| Figure 38. Hg baseline in N <sub>2</sub> and its concentration in N <sub>2</sub> passed through O <sub>2</sub> -treated carbon black bed at 140 °C..... | 64 |
| Figure 39. Effects of HCl on Hg uptake by carbon black in different gases at 140 °C ....  | 65 |
| Figure 40. Effects of SO <sub>2</sub> on Hg uptake by carbon black in HCl + N <sub>2</sub> + CO <sub>2</sub> + O <sub>2</sub> at 140 °C .....           | 66 |

## **ACKNOWLEDGEMENTS**

I would like to thank my Academic Advisor, Dr. Radisav D. Vidić, for advising and supporting me throughout my course of study. His great teaching skills and passion for research have always encouraged me throughout my graduate studies. I would also like to acknowledge other committee members, Dr. Götz Vesper and Dr. Jason D. Monnell, for their comments and assistance with my thesis. I appreciate all of the professors in the Department of Civil and Environmental Engineering at University of Pittsburgh; especially Dr. Amir Koubaa for being a great academic advisor and offering me career advice.

A special thank you goes to Mr. Albert Stewart from the Department of Mechanical Engineering and Material Science and Dr. John Baltrus from the National Energy Technology Laboratory of the U.S. Department of Energy for SEM-EDAX and XPS analysis. I appreciate the assistance from the machine shop at the School of Engineering and the glass shop at the Department of Physics and Astronomy.

I also want to thank my senior Mr. Wenguo (Wayne) Feng for his continuous help on my research and career development. I thank Mrs. Chantal Blake for her company in the office, her help with my English speaking and writing, and sharing her thoughts about life with me. Thanks also go to colleagues and friends, Ana Maria Benavides, Colleen Daley, Huixing Li, Ravi Bhardwaj, Wei Sun, Weizhe and Zhe (Richard) Zhang; they

made my life in graduate school enjoyable. I'm also grateful to my friends in the Chinese community of Pittsburgh, especially my friends from the volleyball club, for their care about my daily life and study.

This work was funded in part by the National Energy Technology Laboratory of the U.S. Department of Energy under Contract No. DE-FG26-05NT42534.

Last, but not least, I would like to thank my parents for their endless encouragement and support during all these years.

## 1.0 INTRODUCTION

Mercury (Hg) is a heavy metal existing naturally in the air, water and soil. Mercury in the air will eventually deposit into the water, or onto the land where it can be washed into water too.<sup>1</sup> Certain anaerobic microorganisms can convert elemental mercury to a highly toxic form, methylmercury. Besides methylmercury, elemental mercury and its other compounds also present great health concerns. Therefore, uses and releases of mercury are regulated in many countries. Coal fired utility boilers are the largest anthropogenic mercury emission source and account for about one-third of mercury emission (50 tons/yr) from combustion point sources in the U.S.<sup>2</sup> On March 15, 2005, EPA issued the Clean Air Mercury Rule (CAMR) to permanently cap and reduce mercury emissions from coal-fired power plants. CAMR makes development of mercury control technology more urgent and also stimulates the research activities in this field. Advances in mercury control technology will highly depend on understanding chemical mechanisms of mercury oxidation and capture.

During coal combustion, mercury is released entirely in the elemental form ( $\text{Hg}^0$ ). Under post-combustion conditions, transform occurs to mercury.<sup>3</sup> A portion of mercury is converted to oxidized mercury ( $\text{Hg}^{2+}$ ) and particle-bound mercury ( $\text{Hg}_p$ ) due to temperature changes, interaction with flue gas components and other combustion products, such as fly ash.  $\text{Hg}^0$  is difficult to remove because of its high volatility and low

solubility. On the other hand,  $\text{Hg}^{2+}$  and  $\text{Hg}_p$  can be easily removed by current existing air pollution control devices (APCDs), such as wet scrubbing systems, electrostatics precipitators, baghouses, etc. So oxidizing mercury and removing it by current APCDs could be a promising mercury approach. There are three potential mechanisms of mercury oxidation: gas phase oxidation, fly ash mediated oxidation and oxidation on catalysts used for selective catalytic reduction (SCR). Homogeneous oxidation is well understood. However, mercury oxidation based on gas phase reaction cannot entirely account for mercury transformations in coal combustion systems. Heterogeneous oxidation is commonly believed to be more important. Post combustion  $\text{NO}_x$  control with SCR may oxidize some mercury. The presence of fly ash has been shown to promote mercury oxidation and adsorption. However, the effects of fly ash on mercury oxidation and adsorption are not well understood yet.

The scope of this study is to understand the impact of fly ash on mercury oxidation and adsorption. The specific objectives are to:

1. Study the physical and chemical properties of different fly ash samples;
2. Investigate the effects of fly ash characteristics on mercury adsorption and oxidation in simulated flue gas and identify the key characteristics and components of fly ash which are responsible for catalyzing mercury transformation;
3. Exam the interaction between flue gas constituents and key fly ash components and their effects on mercury adsorption and oxidation.

## **2.0 LITERATURE REVIEW**

### **2.1 MERCURY TRANSFORMATION IN GAS PHASE**

Mercury transformation under homogeneous conditions was studied by several researchers using both theoretical and experimental studies. It was concluded that both temperature and gas composition are important parameters for mercury speciation.

EPA's Information Collection Request (ICR) data showed that mercury speciation leaving the furnace was principally influenced by coal chlorine content and temperature. The percentage of mercury leaving the furnace in elemental form on average dropped sharply from over 85% to about 10% for coal chlorine content greater than 150-200 ppm (dry basis). NO<sub>x</sub> control had no evident effect on this transformation. The level of mercury oxidation at the exit of the boiler was increased at higher coal chlorine content and lower exit temperature.<sup>4</sup>

Thermodynamic calculations also predicted that mercury oxidation is more favorable at lower temperature. As mercury leaves the combustion zone, the temperature of flue gas cools and equilibrium product shifts from Hg<sup>0</sup> to Hg<sup>2+</sup>. The equilibrium speciation of mercury is influenced by HCl concentration as shown in Figure 1.

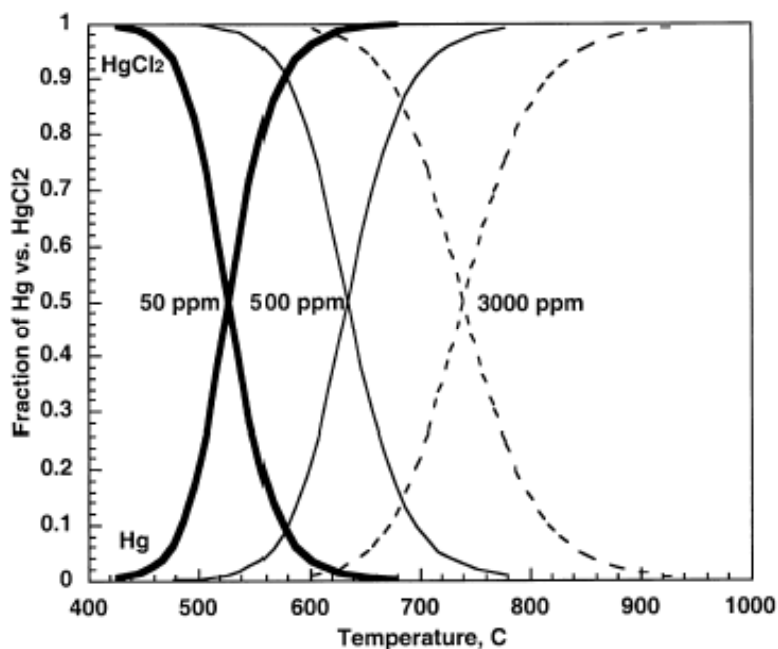


**Figure 1. Equilibrium distribution of elemental and oxidized mercury from various HCl concentrations<sup>5</sup>**

As indicated in Figure 1,  $\text{Hg}^0$  should be almost completely converted to  $\text{Hg}^{2+}$  as flue gas with 50ppm HCl is cooled below 400 °C. However, boilers burning different coals typically show only 35 - 95% oxidation suggesting the conversion process is kinetically controlled.<sup>4</sup>

Many laboratory and theoretical studies have focused on homogeneous transformation of mercury<sup>5-14</sup>, and the results indicate that mercury chlorination is the most important mechanism for mercury transformation in homogeneous systems. Both  $\text{Cl}_2$  and HCl are consistently shown to promote mercury oxidation<sup>5-9, 15</sup>, with  $\text{Cl}_2$  being more effective than HCl. Oxidation of Hg was essentially complete when  $\text{Cl}_2$  concentration reached 10ppm between 20 and 700 °C.<sup>5</sup>



Different reaction pathways were studied in the past. The elemental reaction of  $\text{Hg} + \text{HCl}$  is hindered by a very high energy barrier and can not be considered as an important path under practical conditions.<sup>7</sup> Analysis of 102 elementary reactions identified the predominant reactions to be the oxidation of  $\text{Hg}^0$  by atomic Cl to yield labile  $\text{HgCl}$ , followed by the oxidation of  $\text{HgCl}$  by  $\text{Cl}_2$  to produce  $\text{HgCl}_2$  with associated regeneration of atomic Cl, as indicated in Reactions 1 and 2.<sup>9</sup> Theoretical analyses indicated that oxidation is due to Reactions 1 and 4.<sup>5</sup> Cl atom is believed to be the most dominant oxidizing species.



The low energy barrier reaction involving Cl atom, Reaction 1, proceeds at room temperature. The reaction rate was predicted to be related to Cl,  $\text{Cl}_2$  and HCl concentration. Modeling results from Sliger et al. indicated that the oxidation is limited to temperatures between 700 to 400 °C, which is defined by the overlap of (1) a region of significant superequilibrium Cl concentration, and (2) a region where oxidized mercury is favored by equilibrium. Models developed by Edwards et al.<sup>8</sup> and Xu et al.<sup>10</sup> are also sensitive to temperature change.

Chlorine in coal is released primarily as HCl in the high-temperature zone of a boiler. As the combustion gases cool, HCl is partially oxidized to  $\text{Cl}_2$  by the Deacon process (Reaction 5), which is used industrially to convert HCl to  $\text{Cl}_2$  at temperature between 430 and 475 °C and proceeds only in the presence of a metal catalyst.<sup>16</sup>



As coal chlorine content increases, more of Cl is transformed into Cl<sub>2</sub>. Increases in excess air also increase the Cl<sub>2</sub> transformation. Thermodynamic equilibrium predicts 30 - 60% conversion to Cl<sub>2</sub> for different coals at 150 °C. However, the conversion of HCl to Cl<sub>2</sub> is kinetically limited, as kinetic calculations show that less than 1% of the chlorine is converted to Cl<sub>2</sub>.<sup>7</sup>

Xu et al.<sup>10</sup> developed a kinetic model consisting of 107 reactions and 30 species. Mercury oxidation, as well as chlorination, was included in this model. Reaction 6 was proposed as a significant pathway. 1.5 - 6.0% of the mercury is predicted to be present as HgO. Approximately 10% of the mercury is predicted to be present as HgO by other studies.<sup>5</sup>



Other flue gas constituents (e.g., H<sub>2</sub>O, SO<sub>2</sub>, NO<sub>2</sub>, NO) than may have secondary effects on the rate of homogeneous oxidation of mercury.<sup>7</sup> The interference between these gases and chlorine species may be significant. The extent of mercury oxidation substantially reduced to 25% in flue gas with 10ppm of Cl<sub>2</sub> at 500 °C.<sup>5</sup> Generally, it is believed that SO<sub>2</sub>, H<sub>2</sub>O, and NO inhibit mercury oxidation, and that O<sub>2</sub> is a weak oxidation promoter.

No homogeneous gas phase reaction of elemental mercury with oxygen occurred during a reaction time of 1 hour in the temperature range 20 - 700 °C.<sup>17</sup> However, Hg reacts with O<sub>2</sub>, if a catalyst, such as activated carbon, is present.<sup>6</sup> Niksa et al.<sup>9</sup> also predicted oxygen as a weak promoter.

As regards NO<sub>x</sub>, a slow reaction between Hg and NO<sub>2</sub> has been noted by Hall et al.,<sup>6</sup> and NO is predicted to either promote or inhibit mercury oxidation, depending on its concentration.<sup>9</sup> Higher quench rates increased mercury oxidation in the presence of NO, whereas without NO, faster quenching rates decreased mercury oxidation. Results from Agarwal et al.<sup>11</sup> indicated that NO inhibits mercury chlorination.

SO<sub>2</sub> has been found to inhibit mercury oxidation.<sup>11</sup> The addition of SO<sub>2</sub> completely eliminates the effect of the Cl<sub>2</sub> (84.8% oxidized Hg) in the absence of fly ash.<sup>15</sup> Two reactions (Reactions 7 and 8) are proposed to explain the inhibitory effects of SO<sub>2</sub> and NO, in which SO<sub>2</sub> and NO react with Cl<sub>2</sub>.<sup>11</sup> The consequences of these reactions are a reduction in the oxidative interactions that take place between Hg and Cl<sub>2</sub>, thus decreasing the amount of Hg oxidation that occurs.



However, results from Zhao et al. indicate that SO<sub>2</sub> and NO only inhibit mercury oxidation in the presence of water vapor.<sup>12</sup> The inhibitory effects on Hg oxidation were further confirmed by the reduction of Hg<sup>2+</sup> back into its elemental form. Reaction mechanisms were proposed as in Reactions 9-12.



Moisture can also be a strong inhibitor of Hg oxidation reactions.<sup>9, 11, 12</sup> It even enhanced the inhibitory effects of SO<sub>2</sub> and NO.<sup>12</sup> Other than Reactions 9-12, the effects of moisture could be explained by the reverse reaction of the Deacon Process (Reaction 5).<sup>13</sup>

Mamani-Paco et al.<sup>18</sup> suggested that literature reports of homogeneous mercury oxidation at near ambient temperature likely resulted from catalytic surface effects. Their results suggested that higher concentrations of gaseous HCl or Cl<sub>2</sub> than those found in coal combustion gases are likely required for significant oxidation of mercury to occur by homogeneous reactions alone and that more emphasis should be placed on heterogeneous reaction mechanisms in future studies. Senior et al. noticed that the levels of mercury oxidation predicted by their homogeneous model, while of comparable magnitude to field observations, are still 40 - 80% below oxidation typically observed in field measurements.<sup>7</sup> Therefore, it is very likely that heterogeneous reactions also contribute to mercury oxidation in coal combustion systems.

## **2.2 MERCURY TRANSFORMATION IN HETEROGENEOUS SYSTEMS**

Several reviews<sup>3, 4, 19 20, 21</sup> focusing on mercury transformation in coal-fired power plants indicated that homogeneous reactions could not account for all the mercury transformation in coal combustion systems. Heterogeneous reactions play a very important role in mercury speciation, especially the catalytic oxidation of mercury on fly ash surfaces. In heterogeneous systems, mercury speciation has shown to be influenced by coal constituents such as Cl, S, Se, etc., presence of fly ash and its physical and

chemical characteristics, flue gas components, and operating conditions, including combustion regime, temperature profiles, existence of different APCDs, etc.

### **2.2.1 Coal Composition**

Western subbituminous coals on average contain only about half the amount of mercury and less chlorine and sulfur as compared to Appalachian bituminous coals.<sup>4</sup> The higher chlorine content in Appalachian bituminous coals promotes Hg oxidation and results in a higher percentage of mercury capture by APCDs in coal-fired power plants,<sup>4, 20, 22</sup> as indicated in Figure 2. However, extents of oxidation were not proportional to coal-Cl levels,<sup>23</sup> and the abundance of  $\text{Hg}^{2+}$  and  $\text{Hg}_{(p)}$  was generated by coal with Cl content higher than 200ppm.

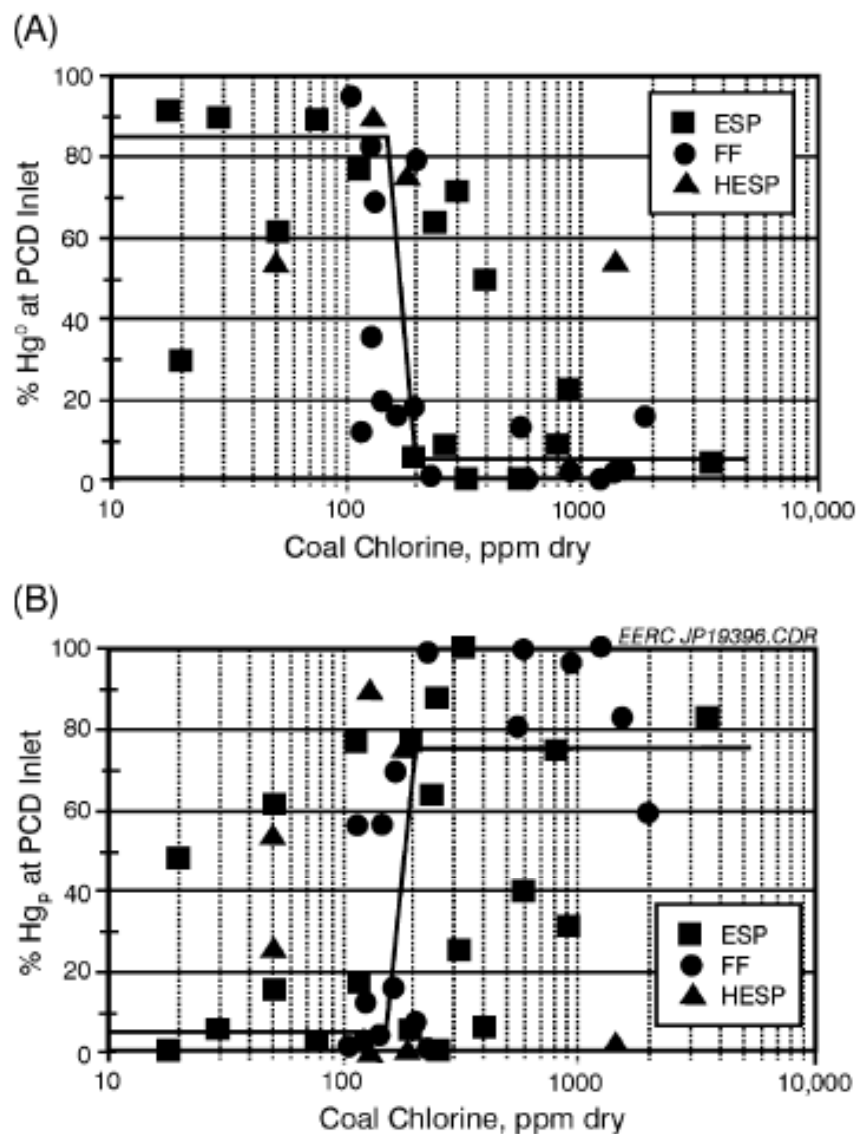


**Figure 2. Percentage of mercury as (A) gas-phase elemental and (B) particulate bound at the inlet of particulate control devices based on ICR data. ESP= Electrostatic Precipitator, FF= Fabric Filter, and HESP=hot-side ESP. Trend lines taken from the ICR data were not statistically determined.<sup>4</sup>**

High sulfur content in coal tends to hinder  $\text{HgCl}_2$  adsorption onto fly ash and results in a high percentage of  $\text{Hg}^{2+}$  in the gas phase.<sup>20</sup> Data from Kellie et al.<sup>22</sup> also

showed a strong relationship between  $\text{Hg}^{2+}$  and coal sulfur concentration. They concluded that sulfur in coal promoted oxidation. However, the high  $\text{Hg}^{2+}$  concentration could be explained by that  $\text{SO}_2$  inhibited adsorption of oxidized mercury onto fly ash.

Hg-Se bonding was found by XAFS and XANES analyses.<sup>24</sup> However, Lopez-Anton et al. found that the presence of selenium in fly ash samples did not have any significant effect on mercury capture.<sup>25</sup>

### **2.2.2 Impact of Fly Ash**

Fly ash not only removes mercury by adsorption, but also promotes mercury oxidation. It catalyzes the reactions between mercury and other flue gas components. Several studies were conducted to investigate the effects of fly ash characteristics on adsorption and oxidation of mercury. The chemical composition of fly ash samples is suggested to be important in catalyzing mercury oxidation as well as adsorbing mercury. Fly ashes from bituminous coal tend to oxidize mercury at a higher degree than fly ashes from subbituminous coals and lignite.<sup>21</sup> No capture of  $\text{Hg}^0$  was observed without accompanying oxidation. Higher mercury oxidation were associated with higher levels of mercury capture.<sup>26</sup> Less mercury oxidation may lead to less mercury uptake.<sup>27</sup> The physical properties, such as surface area, are indicated as a very important factor with respect to mercury oxidation.<sup>28</sup> The interaction between different flue gases and surfaces of fly ash or activated carbon is also important.<sup>28, 29</sup>

It is commonly believed that the oxidation sites are different from adsorption sites, since oxidation continues after 100% breakthrough. Some research suggested that elemental mercury is bound on the carbon in the oxidized form.<sup>24, 29, 30</sup> It is still unknown

what the exact forms of adsorption and oxidation sites are. Heteroatoms, such as Cl, O, N, S, etc. on the edges and corners of the carbon aromatic sheets modify the surface characteristics. Cl sites in particular play an important role in mercury oxidation and adsorption.<sup>4, 30, 31</sup> The addition of halogen atoms to modeled carbon surface has been found to increase activated carbon's capacity for elemental mercury.<sup>32</sup> Increased chloride contents of activated carbon resulted in higher mercury capacity and oxidized mercury in the gas phase.<sup>33</sup> SEM-EDS analysis and XPS results suggested formation of  $\text{HgCl}_2$  on chlorine-impregnated carbon surface.<sup>34</sup> XAFS analysis suggested that captured mercury may be associated with either Cl or S, but that it is likely not associated with oxygen.<sup>24, 29</sup> Oxygen containing surface functional groups reduce mercury uptake by blocking its access to micropores through physisorption; no significant impact of oxygen containing surface functional groups was observed in the chemisorption regime.<sup>31, 35</sup> On the contrary, Li et al. found that both lactone and carbonyl groups appear to be possible active sites for  $\text{Hg}^0$  adsorption, and a higher  $\text{Hg}^0$  capacity is associated with a lower ratio of the phenol/carbonyl groups.<sup>36</sup> Theoretical calculation under simplified conditions indicated that lactone and carbonyl surface functional groups yield the highest binding energies for mercury.<sup>32</sup> It can probably be explained by that mercury is not directly bonded to O atoms; but the resonance effect of the electrons between oxygen surface functional groups and the aromatic rings may stabilize the bindings between other groups and the carbon rings and result in an increase in mercury capture.<sup>37</sup>

Inorganic fractions of fly ash are believed to have little elemental mercury adsorption capacity,<sup>4, 38</sup> although  $\text{HgCl}_2$  has been shown to be captured by  $\text{Ca}(\text{OH})_2$ ,<sup>39</sup>  $\text{CaO}$ ,  $\text{MgO}$  and  $\text{TiO}_2$ .<sup>40</sup> On the other hand, mercury retained in unburned carbon (UBC)



was much higher than in other products separated from fly ash.<sup>41</sup> A positive correlation between UBC content of fly ash, sometimes noted as loss on ignition (LOI), and mercury retention has been demonstrated by different researchers.<sup>4, 38, 42-45</sup> The capacity of fly ash for  $\text{HgCl}_2$  and  $\text{Hg}^0$  are similar<sup>26</sup>, but the adsorption rate is higher for  $\text{HgCl}_2$ .<sup>46</sup> Results from Baltrus et al. showed that unburned carbon concentrates from fly ash have properties similar to most carbon blacks.<sup>47</sup>  $\text{Hg}^0$  retention generally increases with the surface area of the carbon in the ash in a linear relation.<sup>26, 38, 45</sup> There is also a positive correlation between surface area and carbon content in fly ash.<sup>48</sup> However, activated samples have lower capacity than their precursor fly ash or char, although the surface areas are larger. Such behavior suggests that surface area itself is not as critical to mercury capture as the surface functional groups decomposed during the activation processes such as oxygen containing functionalities, F species,  $\text{Cl}^-$  and  $\text{SO}_4^{2-}$  salts.<sup>43, 49</sup>

Fly ash mediated oxidation is an important mechanism for mercury oxidation. Some of the fly ash components promote oxidation of elemental mercury, while some others do not. Ghorishi et al.<sup>50</sup> studied the effects of synthetic model fly ash components on mercury speciation. The results showed that transition metal oxides,  $\text{Fe}_2\text{O}_3$  and  $\text{CuO}$ , exhibited significant catalytic activity in oxidation of  $\text{Hg}^0$  in the presence of  $\text{HCl}$  in simulated flue gas.  $\text{CuCl}$  can promote mercury oxidation even without the presence of  $\text{HCl}$  in the gas phase. The Deacon process catalyzed by these metal compounds was proposed to explain the results.  $\text{Al}_2\text{O}_3$ ,  $\text{SiO}_2$ , and  $\text{CaO}$  did not promote mercury oxidation. Furthermore,  $\text{CaO}$  inhibited  $\text{Hg}$  oxidation probably by removing  $\text{HCl}$ . In addition,  $\text{CaO}$ ,  $\text{MgO}$  and  $\text{TiO}_2$  can promote the conversion of  $\text{HgCl}_2$  to  $\text{Hg}^0$  in flue gas, with  $\text{CaO}$  having the highest conversion rate, while  $\text{Al}_2\text{O}_3$ ,  $\text{SiO}_2$ , and  $\text{Fe}_2\text{O}_3$  do not

promote the conversion.<sup>40</sup> It can be concluded from these two studies that  $\text{Al}_2\text{O}_3$  and  $\text{SiO}_2$  are inert. Iron oxide was suggested to be active in mercury oxidation by Dunham et al.<sup>26</sup> in a study on sixteen different fly ash samples and their interactions with mercury. However, Norton et al. suggested that iron-rich fly ash phases are not necessarily highly catalytic.<sup>28</sup> Two kinds of  $\text{Fe}_2\text{O}_3$  were studied by Galbreath et al.<sup>51</sup> Injection of  $\alpha\text{-Fe}_2\text{O}_3$  did not significantly change Hg speciation; whereas the addition of  $\gamma\text{-Fe}_2\text{O}_3$  improved mercury adsorption as well as oxidation. This suggests that the catalytic effects of  $\text{Fe}_2\text{O}_3$  may be limited to  $\gamma\text{-Fe}_2\text{O}_3$ . Iron catalysts have been tested at both the laboratory and pilot scales for mercury oxidation and shown 10 - 90% oxidation under different conditions.<sup>27</sup>  $\text{TiO}_2$  itself does not exhibit catalytic activity by itself except under ultraviolet radiation.<sup>4</sup> Other than oxides, carbon sites in fly ash are also believed to be responsible for Hg oxidation.<sup>27</sup> Extent of mercury oxidation was found to be correlated with the level of UBC.<sup>23</sup> Considerable oxidation occurred with a high-carbon subbituminous fly ash without magnetite, which also may be caused by UBC in the ash.<sup>26</sup>

### **2.2.3 Impact of Flue Gas Components**

Mercury speciation not only depends on coal type and its composition, but also depends on flue gas composition. There appear to be interactions between flue gas components and fly ash, and interactions between different gas components as well. The effects of different gases are similar to those observed in gas-phase homogeneous studies. Chlorine species ( $\text{Cl}$ ,  $\text{Cl}_2$ , and  $\text{HCl}$ ) have the most dominant effects on Hg oxidation and adsorption. Gases like  $\text{SO}_2$ ,  $\text{H}_2\text{O}$ , and  $\text{NO}$  are believed to inhibit the oxidation and adsorption of Hg.  $\text{NO}_2$  promotes oxidation; but its effect on adsorption is not consistent

among different studies. The effects of flue gas components on mercury oxidation are much more complicated in heterogeneous system than in homogeneous system.

### 2.2.3.1 Hydrogen Chloride (HCl)

HCl was found to enhance mercury adsorption onto carbon surface and promote oxidation of elemental mercury. At low concentration of HCl, essentially  $\text{Hg}^0$  capture onto carbon is little and less than  $\text{HgCl}_2$ . As the HCl concentration increases from 0 to 100 ppm, carbon capacity for both  $\text{Hg}^0$  and  $\text{HgCl}_2$  increases. However, the capacity for  $\text{HgCl}_2$  (500 – 1500  $\mu\text{g Hg/g C}$ ) does not increase as dramatically as the capacity for elemental mercury (0 – 3000  $\mu\text{g Hg/g C}$ ).<sup>46</sup> Galbreath et al. found that injection of HCl into flue gas can convert  $\text{Hg}^0$  to  $\text{Hg}^{2+}$  and / or  $\text{Hg}_{(p)}$ .<sup>51</sup> Kellie et al. also found that increase in HCl concentration can reduce gas phase mercury concentration.<sup>22</sup> A mechanism was proposed to explain adsorption of oxidized mercury species in an excess of chlorine as shown in Reaction 13.<sup>52</sup>



An enhancement in mercury capture by carbonaceous surface could be associated with the formation of carbon-chlorine sites, as the surface chlorine concentration was observed to rise upon exposure of carbon to HCl evidenced by X-ray fluorescence (XRF) analyses.<sup>39</sup> An alternative oxidation mechanism has been proposed for much lower temperatures by Sliger et al.<sup>5</sup> that Cl is catalytically generated by the interaction of HCl with fly ash and char. Once formed, the Cl rapidly reacts with the Hg by Reaction 1, and

the oxidized mercury is partially captured. A similar but more detailed mechanism was proposed by Fujiwara et al. as follows,<sup>23</sup>



where StSA(s) denotes an unoccupied site and StCl(s) denotes a chlorinated site.

### 2.2.3.2 Sulfur Dioxide (SO<sub>2</sub>)

SO<sub>2</sub> has little effects on mercury capture and oxidation by itself.<sup>15, 28, 53</sup> However, its interaction with other gases are important.<sup>28, 53</sup> SO<sub>2</sub> decreases adsorption capacity for both elemental and oxidized mercury in the presence of HCl,<sup>46</sup> and the inhibitory effect is even more severe in the presence of NO<sub>2</sub>.<sup>53</sup> Introduction of SO<sub>2</sub> to an activated carbon previously exposed to NO<sub>2</sub> + Hg caused an immediate Hg breakthrough; the level of mercury concentration in the effluent reached as twice as the inlet, and the desorbed mercury was primarily in the oxidized form.<sup>53</sup> The results suggested that SO<sub>2</sub> not only decreases the capacity of the sorbent, but also causes the release of initially adsorbed elemental mercury, which adsorbed onto the surface as in the oxidized form. An increase in Hg<sup>2+</sup> concentration was observed with an increase in SO<sub>2</sub> concentration in the flue gas by Kellie et al.<sup>22</sup> A mechanism (Reaction 17) involving an increase in Cl<sub>2</sub> concentration was proposed to explain this phenomenon.<sup>22</sup> Cl<sub>2</sub> is continuously regenerated by Reaction 17, and it keeps oxidizing mercury, though part of the gas phase Hg<sup>2+</sup> (HgCl<sub>2</sub>) is converted to particle bound Hg (HgSO<sub>4</sub>(s)) by this reaction. However, the replacement

of  $\text{Hg}^{2+}$  by  $\text{SO}_2$  from the surface can explain the increase in  $\text{Hg}^{2+}$  too,<sup>53</sup> as discussed above.



X-ray photoelectron spectroscopy (XPS) analyses indicated that existence of  $\text{SO}_2$  inhibited Cl adsorption onto carbon surfaces probably by competing for the adsorption sites, and the presence of  $\text{H}_2\text{O}$  and  $\text{NO}_2$  increased the amount of S on the surface. XPS analyses also indicated that sulfur is converted to S(VI) forms on the surface.<sup>54</sup> Basic surface functional groups on carbonaceous surface are responsible for  $\text{SO}_2$  adsorption. Part of the adsorbed  $\text{SO}_2$  stays as  $\text{SO}_2$ ; part of it is converted to S(VI). In the presence of  $\text{O}_2$  and  $\text{H}_2\text{O}$ , formation of  $\text{SO}_3$  can be followed by its transformation into  $\text{H}_2\text{SO}_4$ , which results in an increase in  $\text{SO}_2$  adsorption rate.<sup>29, 55, 56</sup>

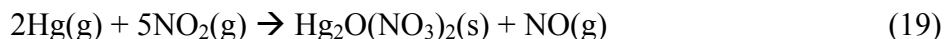
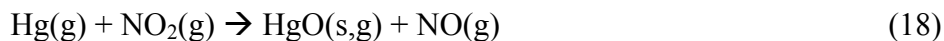
As oxidized Hg could be bound to basic surface functional groups,<sup>4</sup>  $\text{SO}_2$  would compete for the same basic sites with oxidized Hg, which would cause a decrease in mercury adsorption and an increase in oxidized Hg in the gas phase. The presence of  $\text{H}_2\text{O}$  probably inhibits Hg adsorption by accelerating the adsorption of  $\text{SO}_2$ . Effects of  $\text{H}_2\text{O}$  will be discussed later in the water vapor section.

### 2.2.3.3 Nitrogen Oxides ( $\text{NO}_x$ )

The effects of NO and  $\text{NO}_2$  have often been studied together as  $\text{NO}_x$ . The effects of  $\text{NO}_x$  may be related to the ratio of  $\text{NO}:\text{NO}_2$ .<sup>15</sup> Adding  $\text{NO}/\text{NO}_2$  (600/30ppm) can result in more than 25% mercury oxidation with the presence of fly ash. However, the effects disappeared without the presence of fly ash, indicating an interaction between fly ash surface and  $\text{NO}_x$ .<sup>15</sup> The capacity of activated carbon for  $\text{Hg}^0$  decreased as  $\text{NO}_x$  (10% NO

and 90% NO<sub>2</sub>) concentration increased from 0 to 400 ppm in the presence of 50ppm HCl and 1600 ppm SO<sub>2</sub>. Without HCl, the capacity for Hg<sup>0</sup> first increased and then decreased. The capacity for HgCl<sub>2</sub> was not significantly influenced by NO<sub>x</sub> concentration.<sup>46</sup>

Among different flue gases, statistical analyses on full factorial design tests indicated that NO<sub>2</sub> was the most important factor in mercury oxidation in the presence of fly ash.<sup>28</sup> With NO<sub>2</sub> present, oxidation and capture of Hg<sup>0</sup> can occur in the absence of O<sub>2</sub> and HCl. However, no oxidation happens in the absence of HCl and NO<sub>x</sub>.<sup>4</sup> NO<sub>2</sub> probably oxidizes Hg with itself being reduced to NO, as indicated in Reaction 18 proposed by Galbreath and Zygarlicke<sup>57</sup> and Reaction 19 summarized from work by Olson et al.<sup>58</sup>



A synergistic effect between NO<sub>2</sub> and SO<sub>2</sub> was noticed in different studies on mercury oxidation and adsorption.<sup>28, 53</sup> A detailed mechanism was proposed to explain the effects of SO<sub>2</sub> and NO<sub>2</sub> (Figure 3).<sup>4</sup> As shown in Figure 3, HCl, SO<sub>2</sub> and HSO<sub>4</sub><sup>-</sup> could be bound to the basic sites on the surface. NO<sub>2</sub> can act as an electron sink and accept electrons transferred from Hg<sup>0</sup> on the surface, which resulted in oxidation of Hg. Oxidized mercury, such as Hg<sup>2+</sup>, HgCl<sub>2</sub>, Hg(NO<sub>3</sub>)<sub>2</sub> can be bound to basic sites as well. Capture of Hg continues until the binding sites are used up and then breakthrough occurs. In the presence of SO<sub>2</sub>, those sites could be occupied by sulfate where oxidized mercury can no longer be bound.

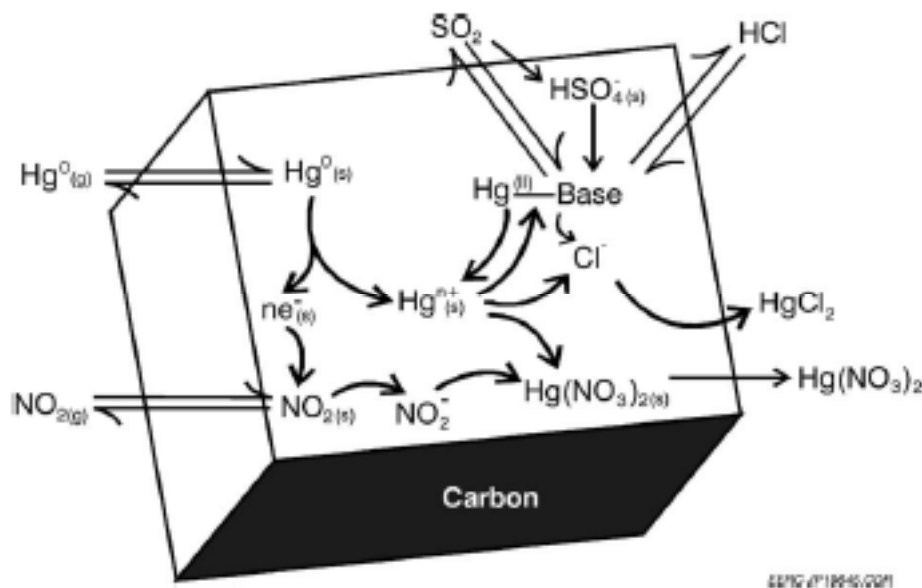


**Figure 3. Suggested heterogeneous model for mercury capture showing potential impact of acid gases<sup>4</sup>**

However, injections of NO<sub>2</sub> (80-190 ppmv) at 440-880 °C into coal combustion flue gases did not significantly affect Hg speciation.<sup>51</sup> This may be due to the difference in residence time and temperature conditions between this combustion system and bench-scale flue gas simulations.

NO tended to suppress mercury oxidation especially when NO<sub>2</sub> was present.<sup>28</sup> The inhibition may be because NO could drive Reactions 18 and 19 to the left.<sup>28</sup> NO has been reported to be adsorbed as NO<sub>2</sub> in the presence of O<sub>2</sub> onto carbon surfaces.<sup>49</sup> No Hg desorption happened while NO<sub>x</sub> was being desorbed from the surface of a NO<sub>x</sub> and Hg loaded activated carbon sample. Besides, no NO<sub>3</sub><sup>-</sup> was detected on the surface. Therefore, it was concluded that Hg and NO<sub>x</sub> were adsorbed to different sites, which conflicts with the model developed by Olson et al.<sup>58</sup>

#### **2.2.3.4 Water Vapor (H<sub>2</sub>O)**

The complete removal of water vapor from flue gas greatly increased the capture of mercuric chloride and produced a smaller increase for Hg; but neither capture was significantly changed by water vapor concentration in the range of 1 – 10%.<sup>46</sup> Reintroducing water into flue gas after a period of sorption testing with dry flue gas results in an immediate release of oxidized mercury from the activated carbon,<sup>4</sup> which indicated that mercury that had been captured in a nonvolatile anhydrous form was subsequently released as volatile hydrate, or oxidized mercury adsorbed on the surface was replaced by the water vapor molecular. On the contrary, carbon surface moisture was found to enhance mercury capture.<sup>35, 59</sup>

### **2.3 SUMMARY AND RESEARCH NEEDS**

Literature review suggests that the heterogeneous reactions are more important than homogeneous reactions for mercury oxidation under post-combustion conditions. The physical and chemical properties of fly ash, flue gas composition, the interactions between them, and operation conditions could all affect mercury oxidation. However, due to the complexity of post-combustion conditions, the mechanisms of mercury oxidation is still not well understood. No specific work has reported an overall evaluation on the effects of these parameters on mercury oxidation and adsorption under post-combustions conditions.



### 3.0 MATERIALS AND METHODS

#### 3.1 SAMPLES

Six ESP hopper fly ash samples were selected for this study. Four of them were collected at four different coal-fired electric utility boilers involved in Department of Energy's field testing programs. They are Southern Company's Gaston Plant, Wisconsin Electric Power Company's Pleasant Prairie Power Plant (PP), and PG&E Corp. National Generating Group's Brayton Point and Salem Harbor (SH) Plant. The coal types and particulate control devices at these power plants are summarized in Table 1.<sup>60, 61</sup> The other two ESP samples were from Consol Energy's field tests with a power plant, whose characteristics are not known. They were named as CE1 and CE2 in this study.

**Table 1 General Characteristics of Power Plants**

| Site             | Coal                  | Particulate Control Device |
|------------------|-----------------------|----------------------------|
| Salem Harbor     | Low sulfur bituminous | Cold-side ESP              |
| Brayton Point    | Low sulfur bituminous | Cold-side ESP              |
| Pleasant Prairie | PRB sub-bituminous    | Cold-side ESP              |
| Gaston           | Low sulfur bituminous | Hot-side ESP, COHPAC FF    |

A carbon black sample, Black Pearls 460 (Cabot Carbon Co., Boston, MA) was used to represent the unburnt carbon in the fly ash samples.

Reagent grade  $\text{Al}_2\text{O}_3$ ,  $\text{CaO}$ ,  $\text{MgO}$ ,  $\text{Fe}_2\text{O}_3$ , and  $\text{TiO}_2$  were used to represent different inorganic compounds in fly ash. Sand (50-70mesh) was used as  $\text{SiO}_2$ .

Unwashed glass beads of 150-212  $\mu\text{m}$  from Sigma – Aldrich were used as a bed support after a pretreatment with aqua regia and half an hour of heat at 500  $^\circ\text{C}$ .

### 3.2 EXPERIMENT SETUP AND PROCEDURE

The impact of fly ash or single synthetic fly ash component was studied in an experiment setup consisting of the following parts: 1) flue gas simulation, 2) mercury generator, 3) reactor and 4) mercury analyzer. A schematic of the setup is shown in Figure 4.

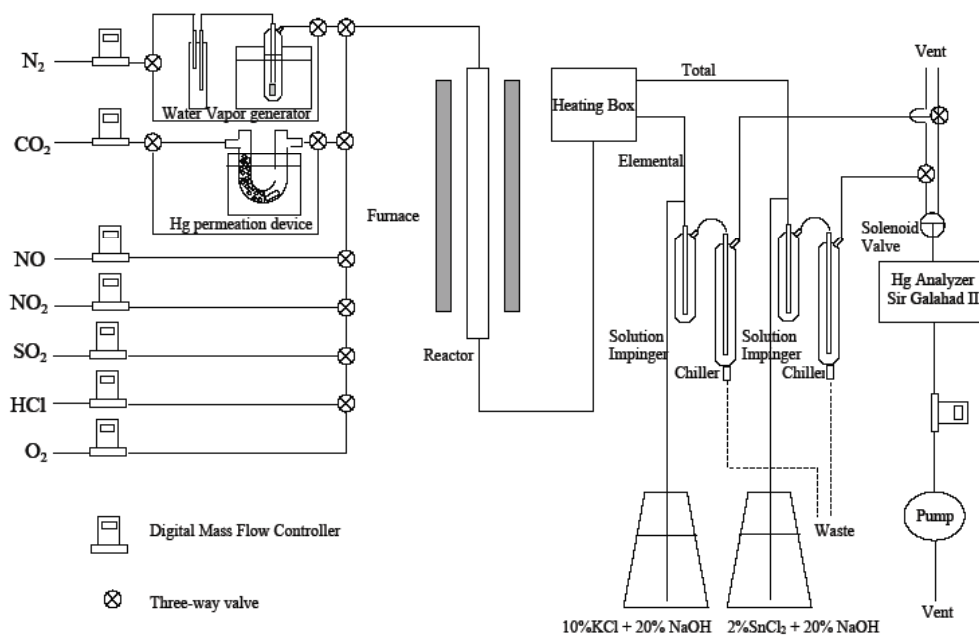


**Figure 4. Schematic of the Hg uptake test setup**

A simulated flue gas consisting of  $\text{N}_2$ ,  $\text{CO}_2$ ,  $\text{O}_2$ ,  $\text{NO}$ ,  $\text{NO}_2$ ,  $\text{SO}_2$ ,  $\text{HCl}$ , and  $\text{H}_2\text{O}$  was generated. A typical bituminous flue gas composition,<sup>15, 26, 28</sup> as listed in Table 2, was

chosen for this study. The total flow rate is 1L/min. Flow rates of different gases were controlled by digital mass flow controllers.

**Table 2 Composition of Simulated Flue Gas**

| Gases              | CO <sub>2</sub> | O <sub>2</sub> | NO      | NO <sub>2</sub> | HCl       | SO <sub>2</sub> | H <sub>2</sub> O | N <sub>2</sub> |
|--------------------|-----------------|----------------|---------|-----------------|-----------|-----------------|------------------|----------------|
| [Feed Tanks]       | 99.99%          | 99.99%         | 3027ppm | 488ppm          | 1022.2ppm | 1.01%           | /                | 99.99%         |
| [Desired]          | 13.5%           | 6%             | 300ppm  | 20ppm           | 50ppm     | 0.15%           | 5%               | Balance        |
| Flow rate (ml/min) | 135             | 60             | 99.1    | 41.0            | 48.9      | 148.5           | 50               | 417.5          |

Water vapor was introduced to the system by sending N<sub>2</sub> to a gas washing bottle, and an empty flask was placed before the water bath in order to prevent backflow of water from entering the setup. Water vapor content was adjusted by adjusting the temperature of water bath.

A mercury permeation tube (VICI Metronics, Santa Clara, CA) was used as the source of elemental mercury. The permeation rate of mercury was designed as a function of temperature only. The tube was seated in a glass U-tube, which was placed in a temperature controlled water bath. Glass beads were placed upstream to facilitate heat exchange.

The 1 L/min simulated flue gas was then fed into a fixed bed quartz reactor (25cm long with 20mm ID), which was placed vertically in a tubular furnace (Lindberg Heavi-Duty, Watertown, WI) with a temperature controller. The effluent stream was then sent to an atomic fluorescence mercury detector to analyze total and elemental mercury concentration.

Mercury analysis system includes a wet conditioning system. Gas first passes through a heating box, which prevents the accumulation of oxidized mercury onto the tubing. The gas is split to two streams; one is directed to the elemental mercury side, and the other is directed to the total mercury side. On the elemental side, 10%KCl + 20%NaOH solution was being pumped to the impinger in order to remove acidic gases and oxidized mercury. On the total side, 2%SnCl<sub>2</sub>+20%NaOH solution was used to reduce oxidized mercury to metallic form and remove acidic gases. After reacting with chemical reagent, the gas carrying spent chemical solution will pass through a chiller, where water vapor is removed from the gas phase.

After the wet conditioning system, mercury in the gas phase is analyzed by PSA 10.525 Sir Galahad II (P S Analytical Ltd, Orpington, Kent, England), a mercury semi continuous emission monitoring (SCEM) system. The instrument is based on atomic fluorescence absorption. During a sampling cycle, gas sample is directed over the gold sand trap, and any mercury will adsorb onto the trap. After that, argon is sent through the trap to flush out any other residual gases, and eliminate their influence on mercury analysis by atomic fluorescence. Mercury is then desorbed from the gold coated sand by heating and carried into the fluorescence detector by argon gas. Lastly, air is supplied to the system to cool it rapidly in preparation for the next analysis cycle.

A timer controlled solenoid valve was used to alternate gas flows to Sir Galahad from elemental and total side. For all the tests in this study, a 200 ml/min flow rate of gas sample was sent to Sir Galahad II during a one-minute sample period. The rest of gas sample was sent to vent after going through an activated carbon trap to remove the toxic gases and Hg.

During a single speciation test, 50mg sample (fly ash, oxides or carbon black) is mixed with 4 g of prepared glass beads and placed on the glass frit in the quartz reactor at a certain temperature.

### **3.3 FLY ASH CHARACTERIZATION**

#### **3.3.1 Surface Area Analysis**

The surface area was measured at 77K using N<sub>2</sub> as adsorbate in the Micromeritics ASAP 2000 apparatus (Micromeritics Instrument Corporation, Norcross, GA). Brunauer-Emmett-Teller (BET) calculation was used to analyze adsorption results and calculate surface area.

#### **3.3.2 Particle Size Distribution Analysis**

The particle size distribution of samples was analyzed with a Microtrac S3500 Tri-Laser particle analyzer (Microtrac Inc., Montgomeryville, PA) using a method built in the software for fly ash sample analysis.

#### **3.3.3 SEM-EDAX Analysis**

SEM (Scanning Electron Microscope) – EDAX (Energy Dispersive Analysis, X-ray) analysis was conducted using a Philips XL30 SEM equipped with an EDAX detector. The SEM analysis yielded information on surface morphology of the fly ash samples,

while the EDAX analysis provided information about surface elemental composition of the fly ash samples.

#### **3.3.4 X-ray Diffraction Analysis**

The powder X-ray diffraction was performed with a Philips X'pert diffractometer to identify crystalline mineral components in fly ash samples. Scans were conducted from 10 to 80° 2 $\theta$  with 0.04° per step each 0.5s.

#### **3.3.5 X-ray Photoelectron Spectroscopy (XPS) Analysis**

Due to the inaccuracy of EDAX results caused by the lack of proper standards, XPS analyses were used to characterize surface chemical properties of fly ash samples. The XPS analyses were carried out using a PHI 5600ci instrument. Monochromatic Al K(alpha) (1486.6 eV) X-rays were used at a power of 400 W, and the analysis chamber was typically maintained at about 10<sup>-8</sup> Torr. The pass energy of the analyzer was 58.7 eV. Samples were analyzed after smearing them on a stainless steel sample holder at a sufficient thickness so that the sample holder could not be detected. Atomic concentrations were calculated using PHI sensitivity factors.

#### **3.3.6 Loss On Ignition (LOI) and Moisture Analysis**

Loss on ignition (LOI) is a standard method to measure unburned carbon in fly ash. The analysis was carried out according to ASTM D3174-82 standard method. First, 2.0  $\pm$

0.5g fly ash sample was weighed and dried at 110 °C for 2 hours, and then cooled in a desiccator for 1 hour. The residual was weighed to calculate the moisture content. Then the sample was heated at 750 °C for 2 hours in a Type F62730 muffle furnace (Barnstead/Thermolyne, Dubuque, IA) and cooled in a desiccator for another hour before being weighed. LOI was calculated as difference in weight and is based the dry basis.

### **3.3.7 TPD Analysis**

Temperature programmed desorption (TPD) of the Carbon black samples tested for mercury uptake under atmospheric pressures was performed under high vacuum. Samples were supported on a Tungsten-grid (W-grid) by pressing them into the W-grid with a hydraulic press. The sample loaded W-grid was mounted with copper clamps on a TPD sample holder connected to a dewar and placed into high vacuum chamber. After evacuation for at least 12 h, the chamber pressure decreased to  $<10^{-8}$  Torr. Then the sample was cooled to cryogenic temperatures ( $\sim 110$  K) and TPD of water dosed from background was performed in the range of temperatures 110-373 K ( $2 \text{ K sec}^{-1}$ ). The water desorption experiment serves as a criterion that the sample and thermocouple are in proper thermal and electrical contact with the W-grid. When the temperature reached 373 K the sample was kept at that temperature for 10 mins to degas physisorbed species. The sample was then allowed to cool down to cryogenic temperature. Liquid nitrogen was removed from the dewar and sample was allowed to heat up spontaneously (to allow condensed gases to evaporate from dewar walls). When the sample reached about 220 to 230 K, the sample was heated ( $2 \text{ K sec}^{-1}$ ) to 1400 K while monitoring desorbing species

in the 1-100 a.m.u. range with a mass spectrometer (RGA 300, Kurt Lesker). For some samples masses were recorded in 1-300 a.m.u. range.



## **4.0 RESULTS AND DISCUSSION**

### **4.1 FLY ASH CHARACTERIZATION**

#### **4.1.1 Surface Area Analysis**

Six fly ashes samples and one carbon black sample (Cabot, Black Pearl 460) were analyzed for surface area, and the results are shown as in Table 3. Salem Harbor fly ash has the highest surface area among the fly ash samples, which makes it of great interest for this study.

**Table 3 Surface Area Analysis Results**

| Sample       | Surface Area<br>(m <sup>2</sup> /g) |
|--------------|-------------------------------------|
| SH           | 17.9                                |
| Brayton      | 5.8                                 |
| Gaston       | 2.1                                 |
| PP           | 3.0                                 |
| CE1          | 2.5                                 |
| CE2          | 1.1                                 |
| Carbon Black | 71.4                                |

#### **4.1.2 LOI and Moisture Analysis**

As depicted in Table 4, Salem Harbor fly ash also has the highest LOI value, which means it has the highest amount of unburned carbon. According to literature findings,

surface area is strongly influenced by carbon content<sup>41</sup> and a positive correlation were found between surface area and carbon content.<sup>48</sup> The results agreed with the literature findings, though the  $R^2$  is not as high as that in the literature. It is mostly probably because the fly ash samples in this study were obtained from different sources.

**Table 4 LOI and Moisture Analysis**

| <b>Sample</b> | <b>LOI%</b> | <b>Moisture%</b> |
|---------------|-------------|------------------|
| SH            | 37.20       | 0.14             |
| Brayton       | 18.06       | 0.12             |
| Gaston        | 11.94       | 0.20             |
| PP            | 0.96        | 0.17             |
| CE1           | 5.97        | 0.07             |
| CE2           | 3.07        | 0.11             |

### 4.1.3 SEM Graphs

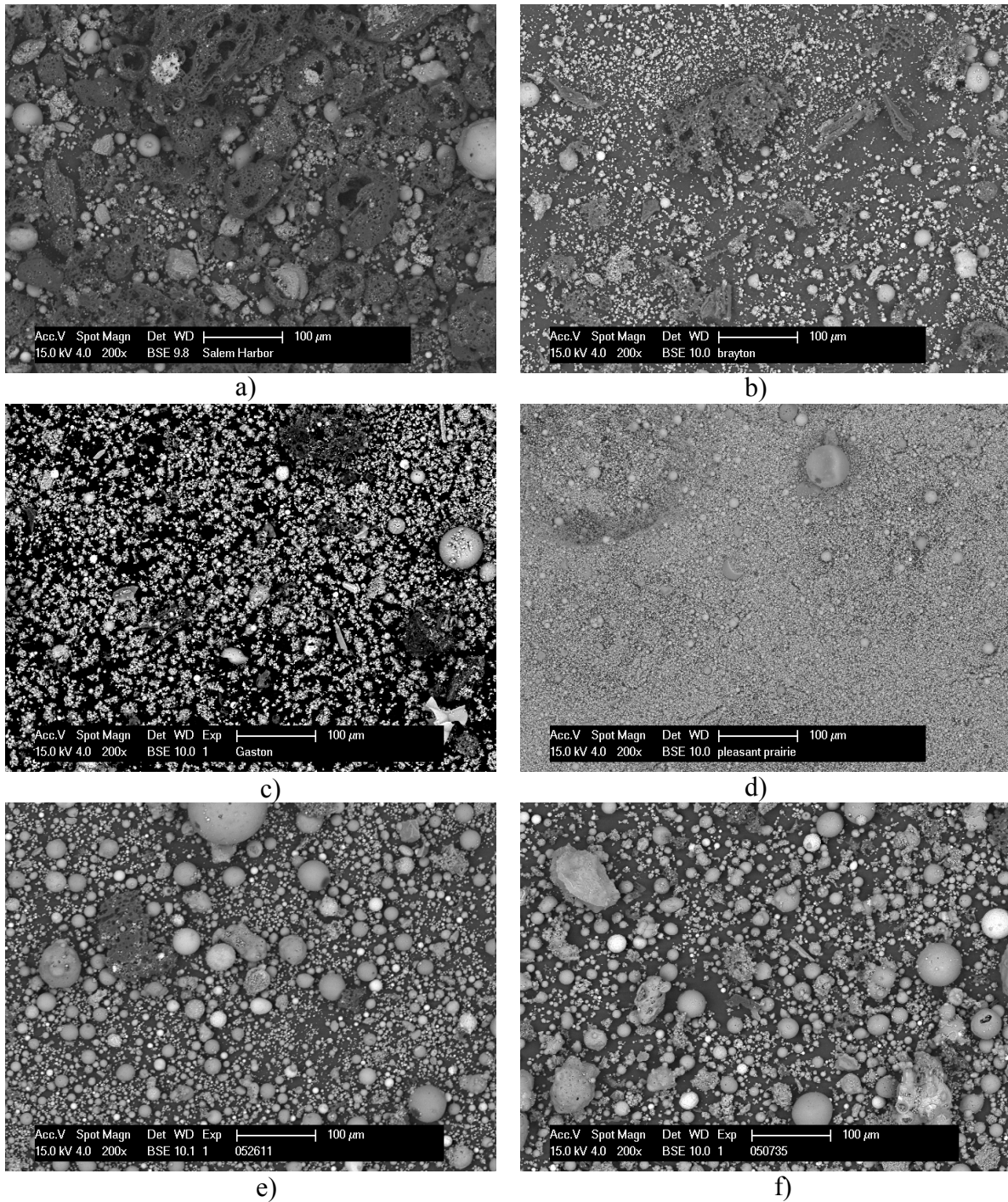


**Figure 5. 200X SEM graphs of fly ash sample a) SH, b) Brayton, c) Gaston, d) PP, e) CE1 and f) CE2**

The above SEM graphs are backscattered images. In a backscattered image, the heavier the atom, the lighter the color. As shown in the images, diverse morphology was found in different samples. Irregular shaped soot (sponge like particles in a)), aluminosilicate glassy spheres, angular quartz, and occasionally mullite spheres were identified by the SEM-EDAX analysis. The relatively high amount of soot present in Salem Harbor (SH) fly ash would account for the high surface area and high LOI.<sup>41</sup>

#### 4.1.4 Particle Size Distribution

Results from a typical size distribution analysis is shown in Figure 6. The particle size falls in a broad range.

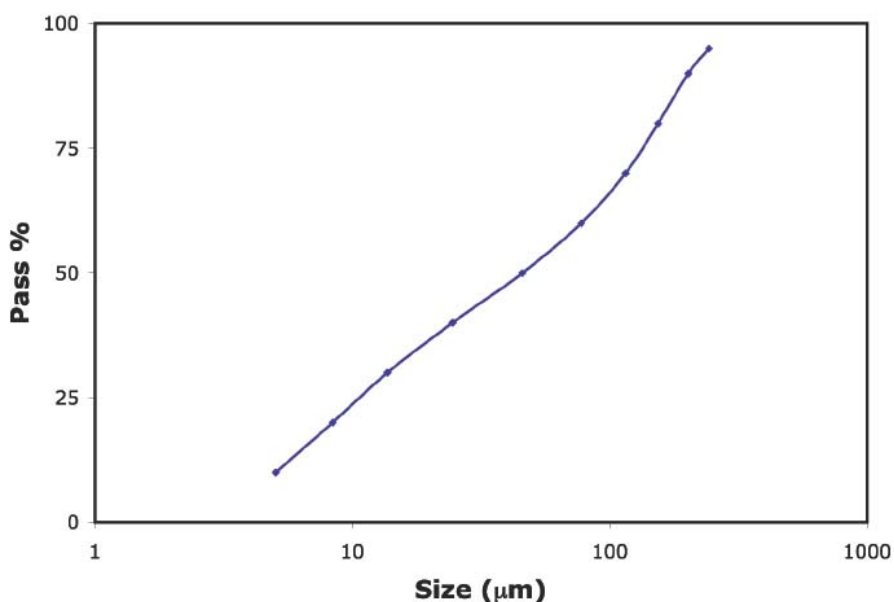


**Figure 6. Size distribution of Brayton Point fly ash sample**

In order to compare different samples, mean particle sizes of these samples are listed in Table 5. The values are higher than those shown in the SEM graphs. It was

mostly caused by the agglomeration of fly ash particles in the circulating water during the analysis process. The high mean particle size of Salem Harbor fly ash is probably due to its high LOI value, since unburned carbon tends to be enriched in coarser fraction in fly ash.<sup>41</sup>

**Table 5 Mean Particle Sizes**

| Sample       | D (μm) |
|--------------|--------|
| SH           | 92.7   |
| Brayton      | 77.6   |
| Gaston       | 30.3   |
| PP           | 48.0   |
| CE1          | 32.7   |
| CE2          | 23.4   |
| Carbon Black | 268    |

#### 4.1.5 Surface Chemical Properties

Table 6 shows the results from EDAX analysis on surface elemental weight percentage.

**Table 6 Surface Elemental Composition from EDAX Analysis on fly Ash Samples**

| Fly Ash | C     | O     | Na   | Mg   | Al   | Si   | P    | S    | K    | Ca    | Ti   | Fe   |
|---------|-------|-------|------|------|------|------|------|------|------|-------|------|------|
| SH      | 74.31 | 16.84 | n.d. | 0.09 | 1.98 | 4.40 | n.d. | 0.27 | 0.41 | 0.56  | n.d. | 1.08 |
| Brayton | 64.80 | 26.23 | n.d. | 0.19 | 2.78 | 3.94 | n.d. | 0.24 | 0.44 | 0.39  | 0.25 | 0.74 |
| Gaston  | 49.20 | 24.94 | 0.31 | 0.28 | 5.72 | 7.62 | 0.27 | 0.93 | 1.24 | 1.30  | 0.81 | 7.38 |
| PP      | 17.17 | 43.26 | 1.37 | 2.61 | 8.42 | 9.37 | 0.76 | 1.59 | 0.39 | 11.68 | 0.76 | 2.63 |
| CE1     | 45.33 | 34.49 | 0.33 | 0.37 | 4.78 | 8.28 | n.d. | 0.45 | 0.72 | 0.86  | n.d. | 4.40 |
| CE2     | 46.82 | 34.8  | 0.18 | 0.22 | 5.6  | 8.17 | n.d. | 0.27 | 0.82 | 0.42  | 0.41 | 2.31 |

n.d. = not detected

Due to the presence of carbon tape, the carbon content in all samples was much higher than suggested by LOI analyses. Further, these results could not be trusted due to insufficient calibration. XPS analysis was then used to give the information on surface chemical composition of these fly ash samples. Table 7 shows the results from XPS analysis.

**Table 7 Surface Elemental Composition (Atom Ratio) from XPS Analysis**

| Fly Ash | C    | O    | N    | Na   | Mg  | Al  | Si   | P    | S   | Ca  | Ti  | Fe  | Mn   |
|---------|------|------|------|------|-----|-----|------|------|-----|-----|-----|-----|------|
| SH      | 54.2 | 31.3 | 1.6  | n.d. | 0.2 | 2.6 | 6.1  | n.d. | 2.4 | 0.6 | 0.1 | 0.8 | n.d. |
| Brayton | 22.7 | 53.8 | n.d. | n.d. | 0.3 | 6.1 | 12.9 | n.d. | 2.4 | 0.5 | 0.2 | 1.0 | n.d. |
| Gaston  | 15.5 | 58.3 | n.d. | 1.7  | 0.5 | 4.5 | 7.7  | 1.0  | 8.8 | 0.8 | 0.2 | 1.1 | n.d. |
| PP      | 10.4 | 56.0 | n.d. | 2.9  | 1.4 | 2.7 | 4.8  | 2.4  | 9.0 | 8.1 | 0.2 | 0.6 | n.d. |
| CE1     | 24.7 | 52.3 | n.d. | 0.6  | 0.1 | 4.7 | 10.7 | n.d. | 4.0 | 1.0 | 0.2 | 1.8 | n.d. |
| CE2     | 24.4 | 51.7 | n.d. | 0.5  | 0.2 | 5.7 | 12.3 | n.d. | 2.8 | 0.7 | 0.2 | 1.5 | n.d. |

n.d. = not detected

Weight Percentage for every element was calculated based on the atom ratio, as shown in Table 8. Compared with the results from EDAX and LOI, results from XPS analyses are more reasonable.

**Table 8 Surface Elemental Composition (Weight Ratio) from XPS Analysis**

| Fly Ash | C    | O    | N    | Na   | Mg  | Al  | Si   | P    | S    | Ca   | Ti  | Fe  | Mn   |
|---------|------|------|------|------|-----|-----|------|------|------|------|-----|-----|------|
| SH      | 41.4 | 31.9 | 1.4  | n.d. | 0.3 | 4.5 | 10.9 | n.d. | 4.9  | 1.5  | 0.3 | 2.9 | n.d. |
| Brayton | 14.9 | 47.1 | n.d. | n.d. | 0.4 | 9.0 | 19.8 | n.d. | 4.2  | 1.1  | 0.5 | 3.1 | n.d. |
| Gaston  | 9.7  | 48.4 | n.d. | 2.0  | 0.6 | 6.3 | 11.2 | 1.8  | 14.6 | 1.7  | 0.5 | 3.2 | n.d. |
| PP      | 6.0  | 43.3 | n.d. | 3.2  | 1.6 | 3.5 | 6.5  | 4.1  | 13.9 | 15.7 | 0.5 | 1.6 | n.d. |
| CE1     | 16.0 | 45.1 | n.d. | 0.7  | 0.1 | 6.8 | 16.2 | n.d. | 6.9  | 2.2  | 0.5 | 5.4 | n.d. |
| CE2     | 15.9 | 44.8 | n.d. | 0.6  | 0.3 | 8.3 | 18.7 | n.d. | 4.9  | 1.5  | 0.5 | 4.6 | n.d. |

According to the elemental analyses, oxides, including MgO, Al<sub>2</sub>O<sub>3</sub>, SiO<sub>2</sub>, CaO, TiO<sub>2</sub>, Fe<sub>2</sub>O<sub>3</sub>, and UBC were selected as fly ash components for tests in flue gas. Carbon

black was used in this study to represent UBC in the samples due to the similarity between UBC in fly ash and carbon black.<sup>47</sup>

## 4.2 MERCURY UPTAKE TESTS

### 4.2.1 Baseline

Figure 7 depicts the results of an experimental with an empty reactor. This run is necessary to establish baseline conditions before introducing solid samples into the system.

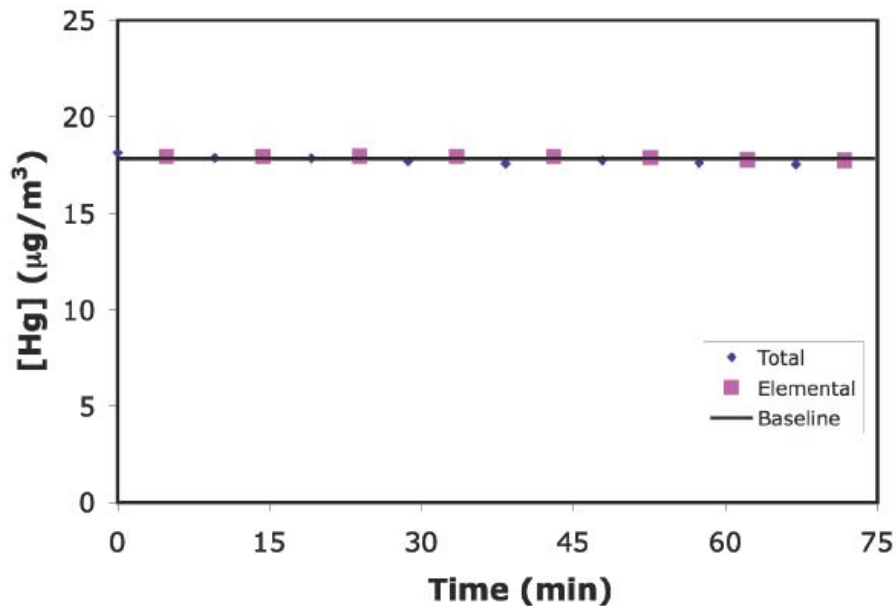
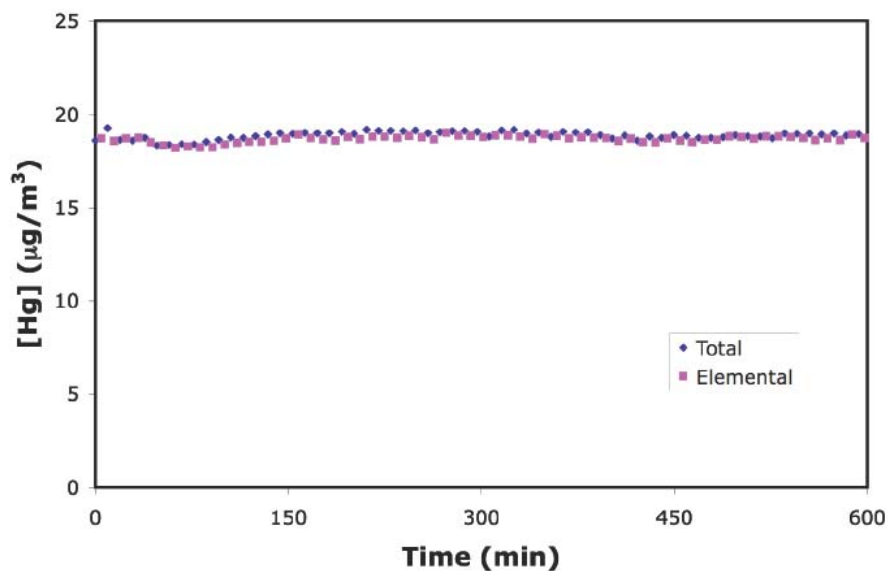


Figure 7. A typical baseline run with flue gas at 140 °C

As shown in Figure 7, there was no difference between elemental and total mercury readings, which means no mercury oxidation occurred at 140 °C under the flue gas conditions in this study. Glass beads were used as a media for suspending fly ash evenly in the reactor and creating certain detention time for the reaction. Experiments with glass beads indicated that pretreated glass beads were inert. In order to verify that the system can stay stable long enough, a 10-hr experiment was carried out with an empty reactor (Figure 8).



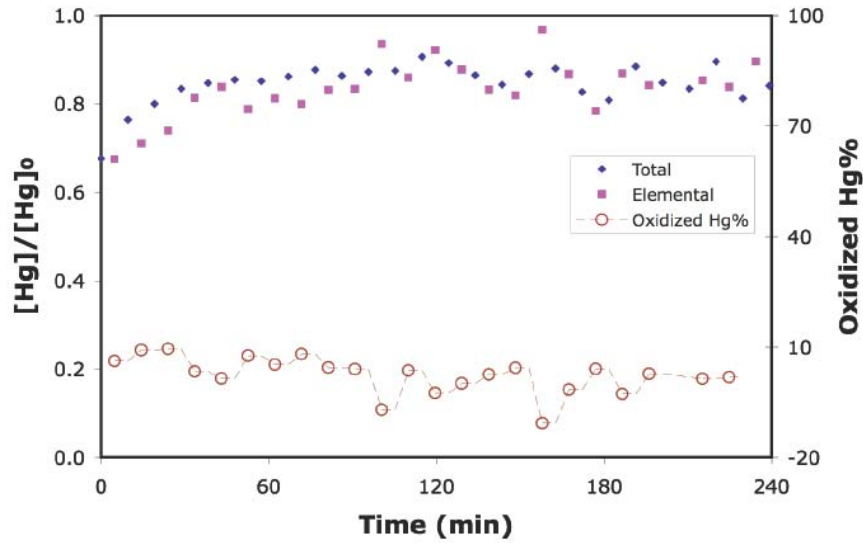
**Figure 8. A 10-hr baseline run with flue gas at 140°C**

The results indicated that the system could be stable for at least 10 hours. For each experiment, a stable mercury baseline like Figure 7 was reached before the introduction of samples into the reactor.



#### 4.2.2 Mercury Speciation Tests with Fly ash samples

The results from mercury uptake tests with the six ESP hopper fly ash samples will be discussed in the section.



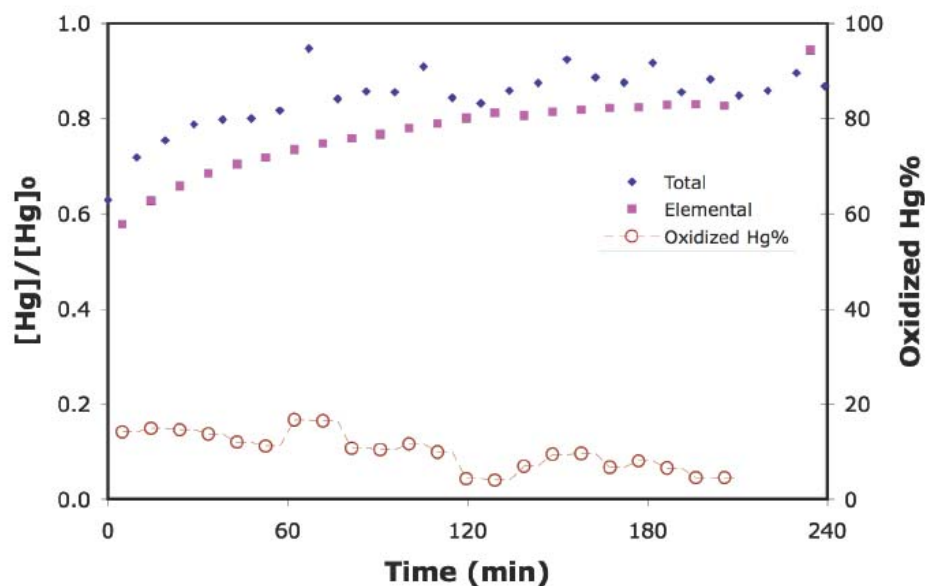
**Figure 9. Hg uptake test with 50 mg CE1 fly ash at 140 °C**

Figure 9 shows the results of mercury uptake test with 50mg CE1 fly ash sample using a simulated flue gas (Table 2). Mercury concentration in the effluent was normalized to the influent concentration, and is shown on the left hand vertical axis. Oxidized Hg percentage was calculated by the following formula:

$$\text{Oxidized Hg\%} = (C_{\text{Total}} - C_{\text{Elemental}}) / C_{\text{Total}} \times 100\%$$

where,  $C_{\text{Total}}$  is the total mercury concentration in the effluent from the reactor, and  $C_{\text{Elemental}}$  is the elemental mercury concentration. Percentage of oxidized mercury is shown on the right hand vertical axis.

After the introduction of CE1 fly ash sample into the reactor, mercury concentration in the effluent dropped to around 70% of the inlet level. As the fly ash sample slowly picked mercury up and lost some of its capacity, the effluent mercury concentration increased. However, there was a difference between elemental and total mercury concentration constantly, which means the CE1 fly ash also has an oxidation capacity for mercury besides adsorption of mercury. The oxidation capacity decreased slightly during the test.



**Figure 10. Hg uptake test with 50 mg CE2 fly ash at 140 °C**

The test with CE2 fly ash showed similar trend. 100% breakthrough was slowly approached, and oxidized Hg percentage decreased gradually.

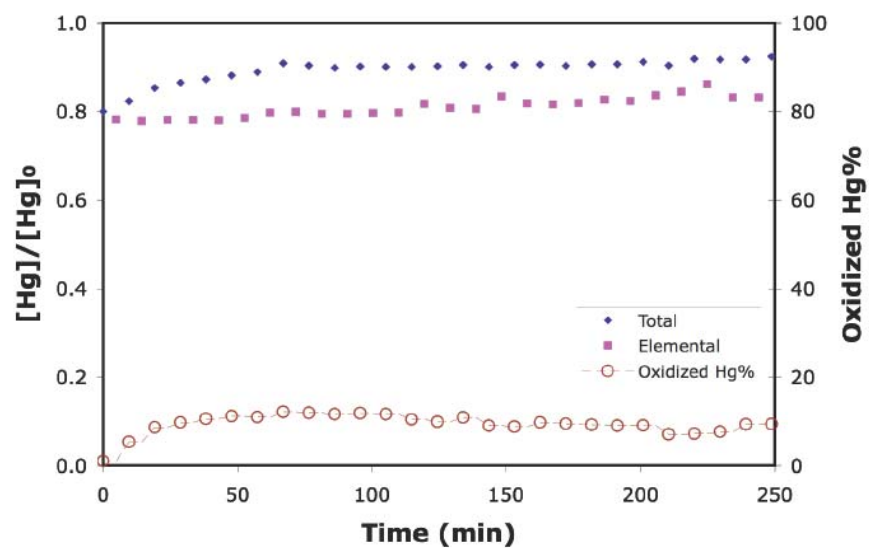


Figure 11. Hg uptake test with 50 mg PP fly ash at 140 °C

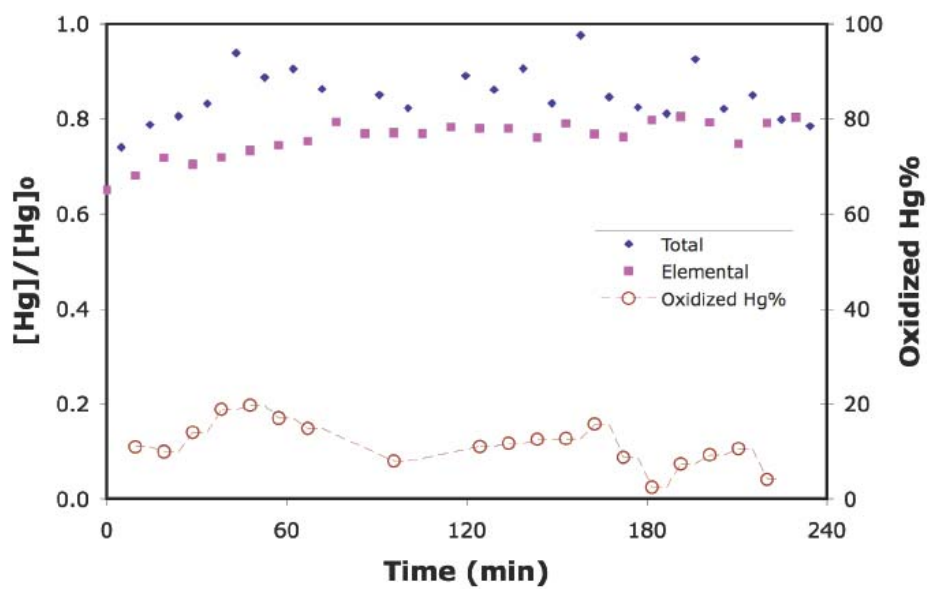


Figure 12. Hg uptake test with 50 mg Gaston fly ash at 140 °C

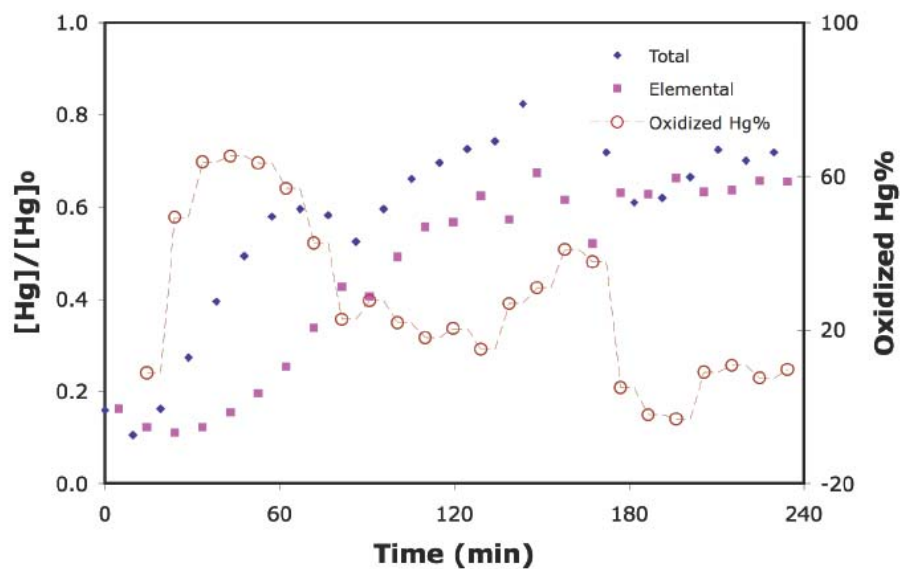


Figure 13. Hg uptake test with 50 mg Brayton fly ash at 140 °C

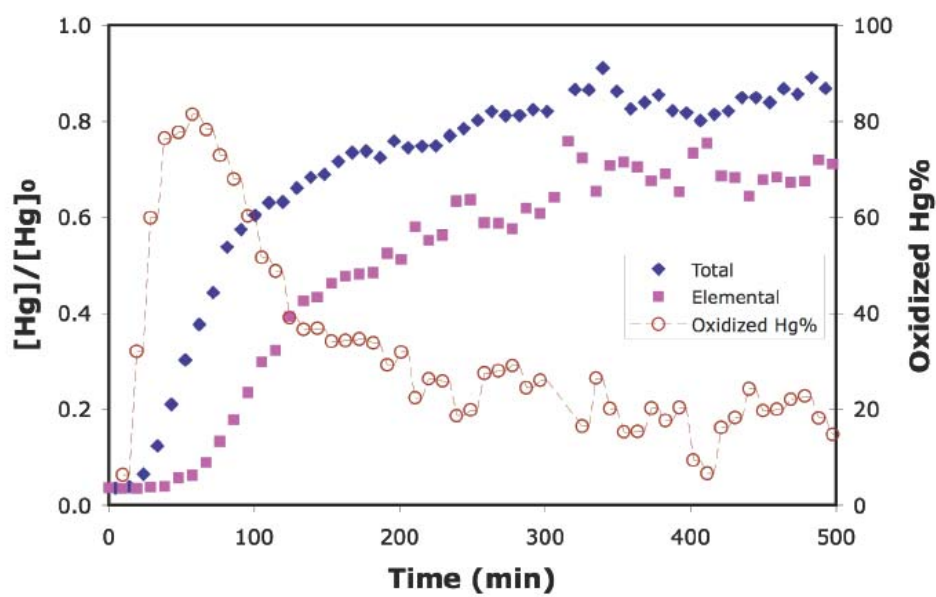


Figure 14. Hg uptake test with 50 mg SH fly ash at 140 °C

Figure 11 - 14 show the results from tests with Please Prairie, Gaston, Brayton Point, Salem Harbor fly ash samples. In summary, fly ash not only captures mercury, but also promotes mercury oxidation. With flue gas itself, mercury stays in elemental form (Figures 7 and 8). After the fly ash sample was introduced to the reactor, part of the  $\text{Hg}^0$  got captured on the surface; part of the Hg left the reactor in either  $\text{Hg}^0$  or  $\text{Hg}^{2+}$  form. The sample slowly reached its maximum capacity, but oxidation still took place. The results with different fly ash samples were different, though the trends were similar, indicating that the adsorption capacity and catalytic oxidation depended on fly ash characteristics. In order to compare the performance of different fly ash samples, mercury load on fly ash and oxidized mercury ratio in the effluent after four hours of exposure were calculated and presented in Table 9.

**Table 9 Hg uptake and oxidation after four-hour exposure with fly ash**

| Sample  | Mercury Load ( $\mu\text{g/g}$ ) | Oxidized $\text{Hg}^0\%$ |
|---------|----------------------------------|--------------------------|
| SH      | 47.9                             | 22.9%                    |
| Brayton | 38.3                             | 9.3%                     |
| Gaston  | 14.6                             | 7.3%                     |
| PP      | 8.8                              | 8.1%                     |
| CE1     | 13.1                             | 1.6%                     |
| CE2     | 13.2                             | 5.2%                     |

Among these samples, the SH fly ash showed the highest capacity for mercury as well as the highest oxidized mercury percentage in the effluent. With the presence of SH fly ash, there was still around 20% of oxidized Hg in the effluent after an 8-hr exposure to flue gas (Figure 14). According to the surface characterization, SH fly ash sample also has the highest surface area. Surface area was found to have positive correlations with

both mercury uptake and oxidation, as indicated in Figure 15. Such findings are in agreement with other studies.<sup>26, 28, 38, 45</sup>

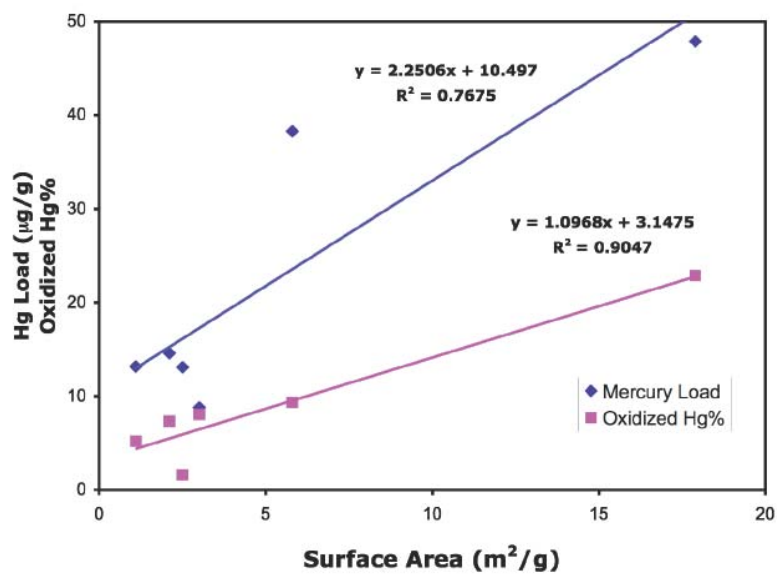


**Figure 15. Effects of surface area on Hg uptake and oxidation at 140 °C**

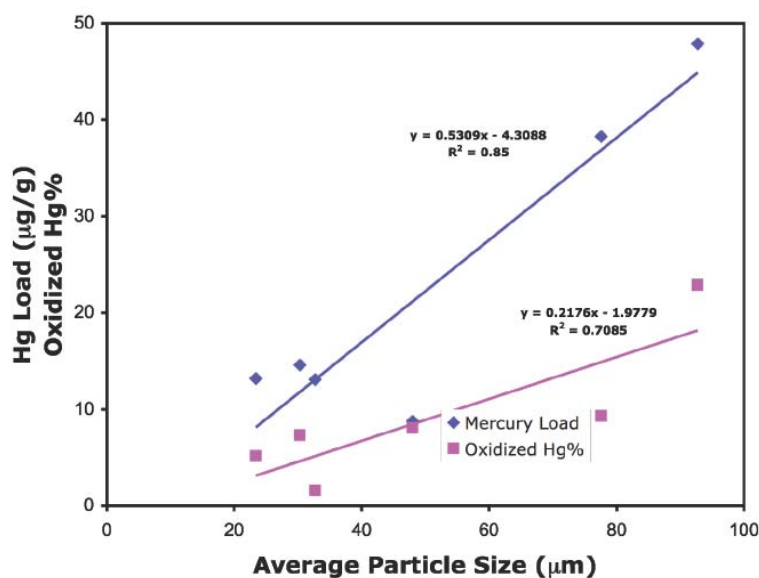


**Figure 16. Effects of particle size on Hg uptake and oxidation at 140 °C**

Other than surface area, the effects of particle size were also studied. Mercury capture and oxidation also increased with particle size (Figure 16). Such findings could be explained by the fact that UBC is enriched in the coarser fractions in the fly ash samples used in this study according to SEM-EDAX analyses and is in agreement with results from Suraez-Ruiz et al.<sup>48</sup> and Hwang et al.<sup>41</sup>

Not surprisingly, Hg load and oxidation were found to be proportional to LOI values (Figure 17), suggesting the unburned carbon is actively involved in both mercury oxidation and adsorption processes. The similarity between effects of LOI, surface area and particle size on Hg load and oxidation is likely due to the fact that carbon has a higher surface area than other fractions<sup>41</sup> and tends to be enriched in coarser fractions in fly ash.<sup>48</sup>

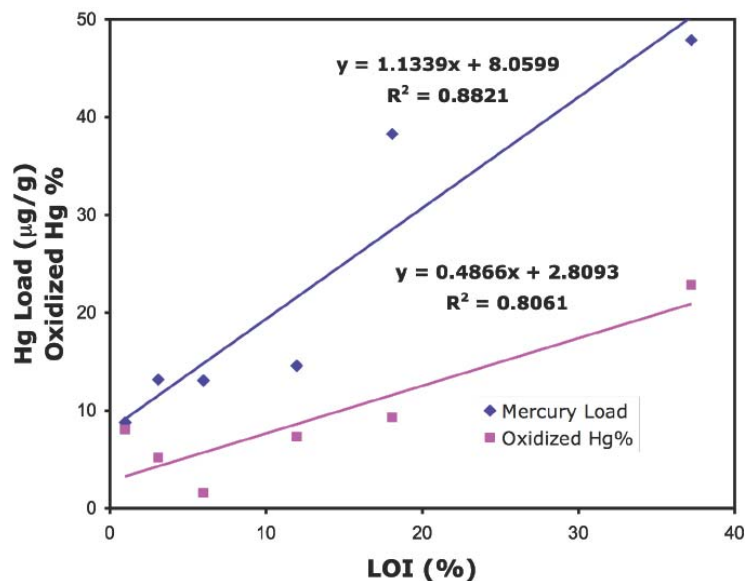


Figure 17. Effects of LOI% on Hg uptake and oxidation at 140 °C

Experiments were done in order to verify whether UBC itself has an important impact as suggested above and to find out what the effects of other components of fly ash are on mercury uptake and oxidation. The results are discussed in the following section.

#### 4.2.3 Mercury Speciation Tests with Synthetic Single Components

Similar uptake tests to the ones with fly ash were performed with carbon black and oxides typically present in fly ash, such as  $\text{SiO}_2$ ,  $\text{Al}_2\text{O}_3$ ,  $\text{MgO}$ ,  $\text{CaO}$ ,  $\text{TiO}_2$ , and  $\text{Fe}_2\text{O}_3$ .

A test with raw sand (White quartz, -50+70 mesh, Sigma-Aldrich, St. Louis, MO) is shown in Figure 18. Raw sand exhibited some mercury uptake and oxidation; however, the pretreated sand (Washed with aqua regia and then burned in the muffle



furnace at 500°C for 30 min) showed almost no oxidation and adsorption (Figure 19), indicating that the oxidation and adsorption is possibly caused by the impurities on sand surface.

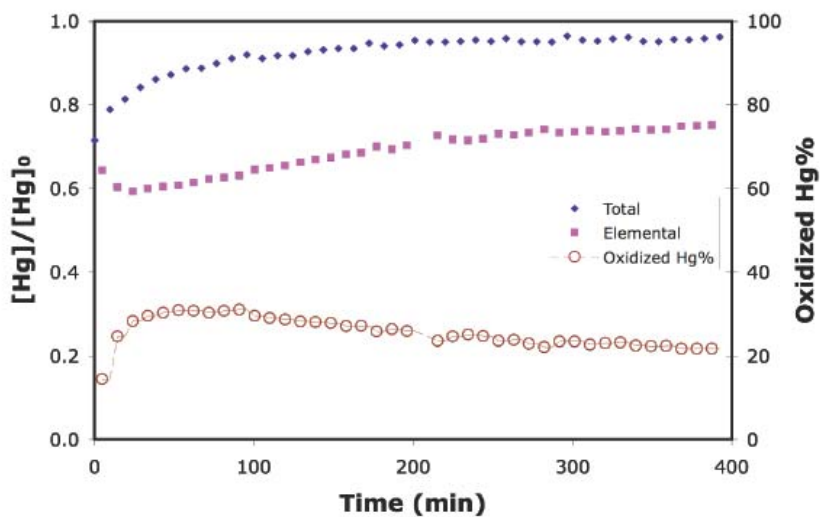


Figure 18. Hg uptake test with 8 g raw sand at 140 °C

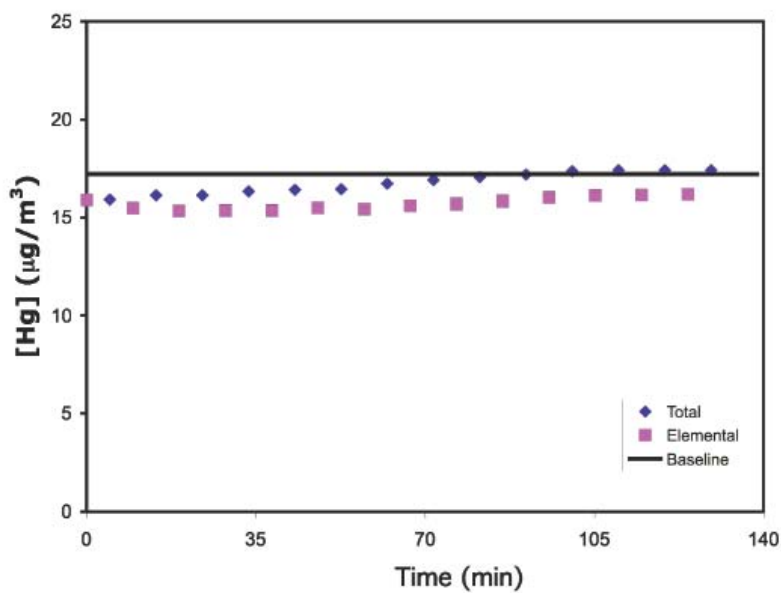
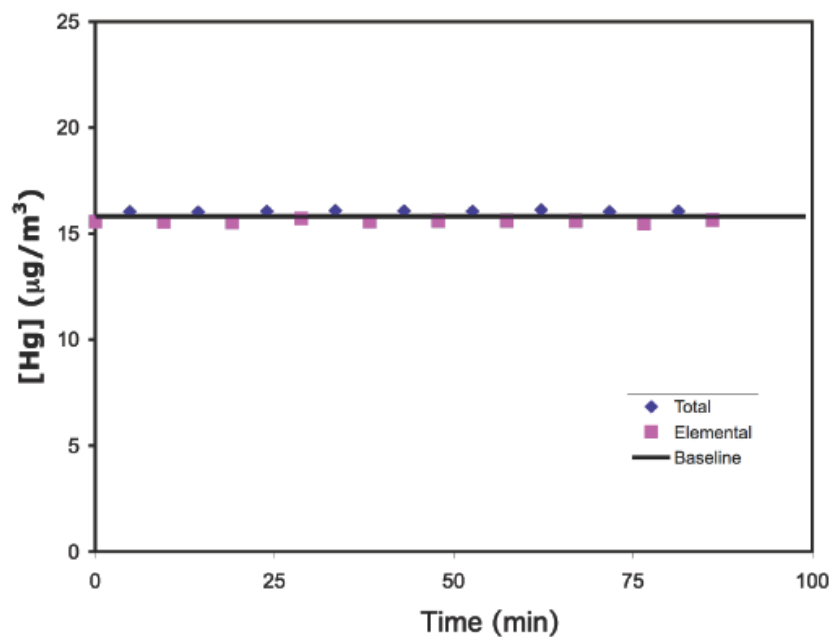


Figure 19. Hg uptake test with 4 g treated sand at 140 °C

Tests with  $\text{Al}_2\text{O}_3$ ,  $\text{MgO}$ ,  $\text{CaO}$ , and  $\text{TiO}_2$  in simulated flue gas (Table 2) showed similar results (Figure 20 - 23) to the one with treated sand. None of these oxides exhibited capacity for oxidizing or capturing  $\text{Hg}^0$ , as shown in the figures that total mercury and elemental mercury readings were the same as the baseline level. Such findings agrees with results from Ghorishi et al.<sup>50</sup> and Thorwarth et al.<sup>40</sup> However, it does not necessarily mean that these oxides have no effects on mercury uptake or oxidation. They may inhibit mercury uptake or oxidation by consuming acid gases like  $\text{HCl}$ , which is especially true for  $\text{CaO}$ .<sup>39, 40, 62</sup>



**Figure 20. Hg uptake test with 50 mg  $\text{CaO}$  at 140 °C**

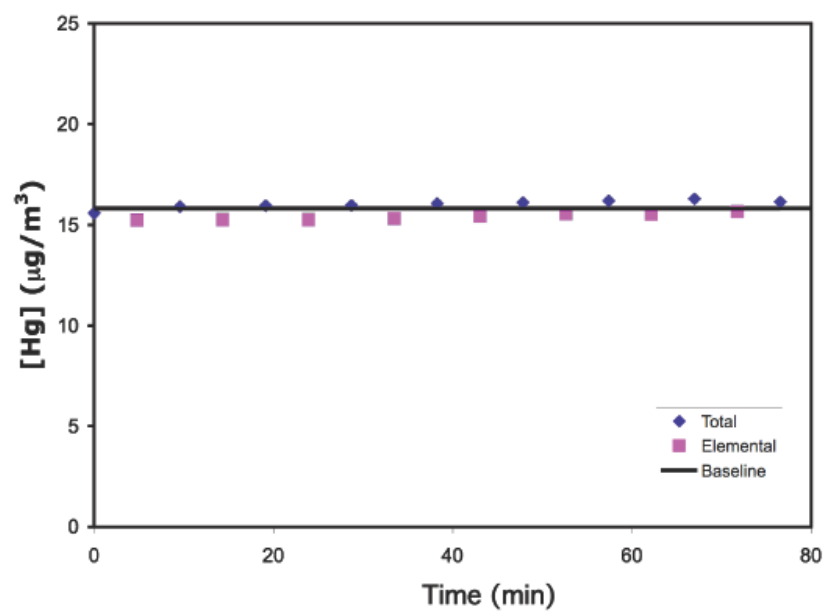


Figure 21. Hg uptake test with 50 mg MgO at 140 °C

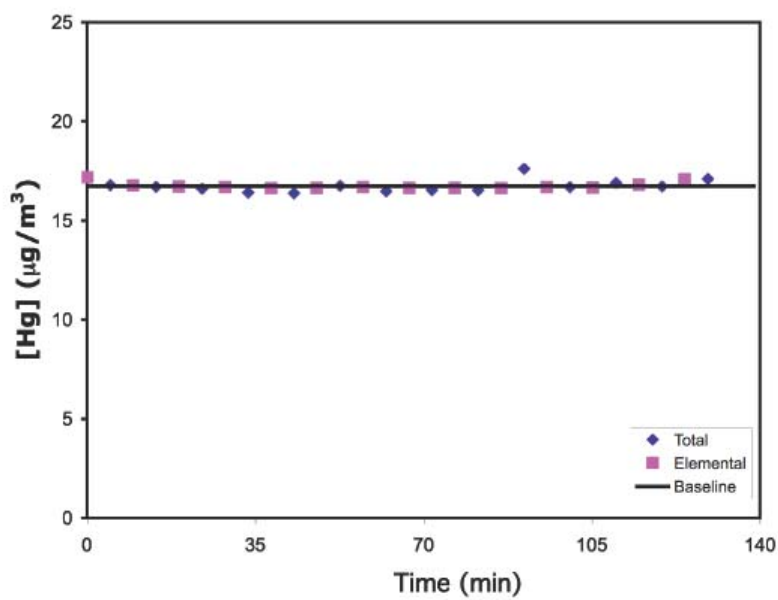
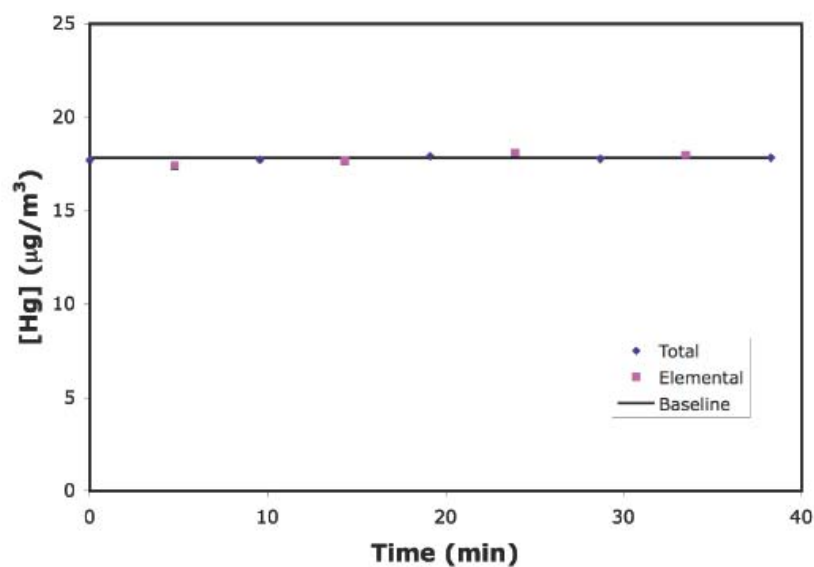
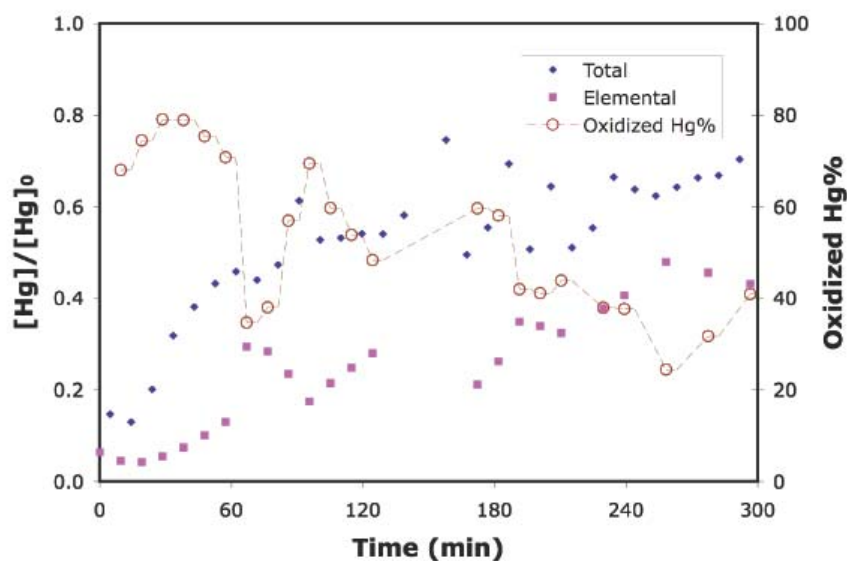


Figure 22. Hg uptake test with 50 mg  $\text{Al}_2\text{O}_3$  at 140 °C



**Figure 23. Hg uptake test with 50 mg TiO<sub>2</sub> at 140 °C**

Ferric oxide showed a significant oxidation capacity at the beginning of the test as shown in Figure 24. Oxidized mercury in the effluent was as high as 80%. As the test proceeded, the oxidation rate decreased to around 40% in four hours. Based on this study, it can be concluded that ferric oxide has a potential to be a mercury oxidation catalyst in flue gas, which has also been suggested by others.<sup>26, 63</sup>



**Figure 24. Hg uptake test with 50 mg Fe<sub>2</sub>O<sub>3</sub> at 140 °C**

Carbon black was used to simulate UBC in fly ash samples. It showed a much higher capacity for adsorbing mercury than the oxides tested in this study (Figure 25). The oxidized mercury was consistently around 20%-30% in the effluent during the 5-hr experiment except for a slight increase in the very beginning of the test. Carbon black showed a remarkable ability to catalyze the oxidation of Hg<sup>0</sup> under the conditions of this study, which explains why mercury uptake and oxidation increased with increases in LOI values. Other studies have also shown that mercury oxidation is related to the extent of UBC.<sup>22, 26, 27, 63</sup>

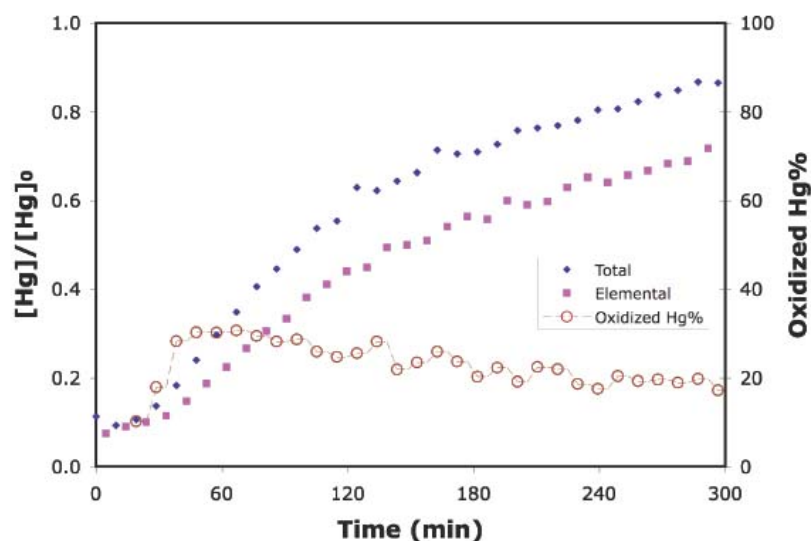


**Figure 25. Hg uptake test with 50 mg carbon black at 140 °C**

Effects of  $\text{Fe}_2\text{O}_3$  and carbon black on mercury oxidation and capture are summarized in Table 10. They showed comparable mercury capture capacity; but, the Hg oxidation capacity of  $\text{Fe}_2\text{O}_3$  is much higher than carbon black. However, carbon content of the fly ash samples used in this study ranged from 10 to 54 Atom%, while  $\text{Fe}_2\text{O}_3$  was only present at 0.6 - 1.5 Atom%. Therefore,  $\text{Fe}_2\text{O}_3$  is relatively less important than UBC for mercury oxidation and adsorption. It could be concluded that unburned carbon is the most important component in fly ash for mercury oxidation and adsorption.

**Table 10 Hg Uptake and Oxidation after Four-hour Exposure with Fly  
Ash Components**

| Sample                  | Mercury Load ( $\mu\text{g/g}$ ) | Oxidized Hg% |
|-------------------------|----------------------------------|--------------|
| $\text{Fe}_2\text{O}_3$ | 42.5                             | 41.00%       |
| C black                 | 39.0                             | 19.44%       |

From all experiments done with oxides, it was concluded that  $\text{Al}_2\text{O}_3$ ,  $\text{MgO}$ ,  $\text{CaO}$ , and  $\text{TiO}_2$  did not promote either mercury oxidation or mercury capture under flue gas conditions in this study. Purified  $\text{SiO}_2$  was able to adsorb and oxidize a small amount of  $\text{Hg}^0$ , but the effects were not significant. Both  $\text{Fe}_2\text{O}_3$  and carbon black showed profound impacts on mercury adsorption and oxidation. Carbon is more important due to its higher amount. However, the SH fly ash sample having a lower carbon content and a lower surface area than carbon black showed comparable capacities for mercury oxidation and adsorption to carbon black, suggesting that the heteroatoms on the fly ash sample and the conditions the fly ash previously exposed to would be important for mercury transformation. It also indicates that the effects of fly ash are more complex than single fly components.

In order to find out the mechanisms of mercury oxidation, the second part of this study focused on carbon part: the interaction between the carbonaceous surface and single flue gas component, the interaction between different gas components, and their effects on mercury adsorption and oxidation.

#### 4.2.4 Mercury Speciation Tests with Carbon Black under Different Flue Gas Composition

In order to exam the effects of different flue gas combination (without Hg) on the surface chemical properties, 50 mg of carbon black sample was exposed to each flue gas combination listed in Table 11 at 140 °C for either 3 hrs (XPS analysis) or about 12 hrs (TPD analysis), and the results from TPD and XPS analyses are summarized in Table 11.

**Table 11 TPD and XPS Analyses of Carbon Black Samples Treated with Different Flue Gas Combination**

| Carbon Black Samples<br>(Flue gas combination)                               | TPD (Desorption temperature) |                 | XPS (Atomic %) |     |     |      |      |
|--|------------------------------|-----------------|----------------|-----|-----|------|------|
|  | CO/CO <sub>2</sub>           | SO <sub>2</sub> | C              | O   | S   | N    | Cl   |
| 0: As-received   |                              | n.d.            | 98.6           | 0.7 | 0.6 | 0    | 0    |
| 1: SO <sub>2</sub> +CO <sub>2</sub> +O <sub>2</sub> +NO <sub>2</sub> +NO+HCl | 600-800 K                    | 400-900K        | 98.2           | 1.0 | 0.7 | 0    | 0.1  |
| 2: HCl+N <sub>2</sub>  | (Signal intensity is on      | n.d.            | 98.8           | 0.6 | 0.6 | n.d. | 0    |
| 3: CO <sub>2</sub> +O <sub>2</sub> +HCl+N <sub>2</sub>                       | the same order of            | n.d.            | 98.4           | 1.0 | 0.7 | n.d. | 0    |
| 4: SO <sub>2</sub> +CO <sub>2</sub> +O <sub>2</sub> +HCl+N <sub>2</sub>      | magnitude)                   | 400-900K        | 98.8           | 0.5 | 0.6 | 0    | 0    |
| 5: SO <sub>2</sub> +CO <sub>2</sub> +O <sub>2</sub> +N <sub>2</sub>          | /                            | /               | 98.4           | 0.9 | 0.7 | n.d. | n.d. |
| 6: NO <sub>2</sub> +N <sub>2</sub>   | /                            | /               | 98.6           | 0.7 | 0.6 | 0    | n.d. |

/ = No analyses; n.d. = not detected.

As illustrated by TPD analyses in Table 11, surface oxygen functionalities were present in all the analyzed samples including the as-received carbon black. SO<sub>2</sub> species was desorbed during the analyses on Samples 1 and 4, which had been exposed to SO<sub>2</sub>. No nitrogen or chlorine related species were desorbed from the surface in the TPD tests. The differences in surface chemical composition between samples 0-6 prepared for XPS analyses were not significant.

Experiments were designed to explore the effects of flue gas composition on mercury uptake. A stable baseline of Hg were reached in either N<sub>2</sub> or N<sub>2</sub> + CO<sub>2</sub> + O<sub>2</sub>. After that, 50 mg carbon black was introduced into the reactor afterwards and mercury in



the effluent was monitored until 100% breakthrough was reached. Then flue gas composition was altered while still keeping a flow rate of 1 L/min, and mercury speciation in the effluent was monitored.

As depicted in Figure 26 and 27, a 100% breakthrough was achieved immediately in either  $N_2$  or  $N_2 + CO_2 + O_2$ . It can be concluded that carbon black itself does not adsorb much elemental mercury. However, TPD analysis of as-received carbon black (Table 11 and Figure 28) revealed the presence of surface oxygen functionalities on these carbon black samples. These results indicated that oxygen functionalities are not able to adsorb mercury or oxidize mercury by themselves, though they may play a role in capturing mercury under conditions that are different from those in experiments shown in Figure 26 and 27.<sup>36</sup>

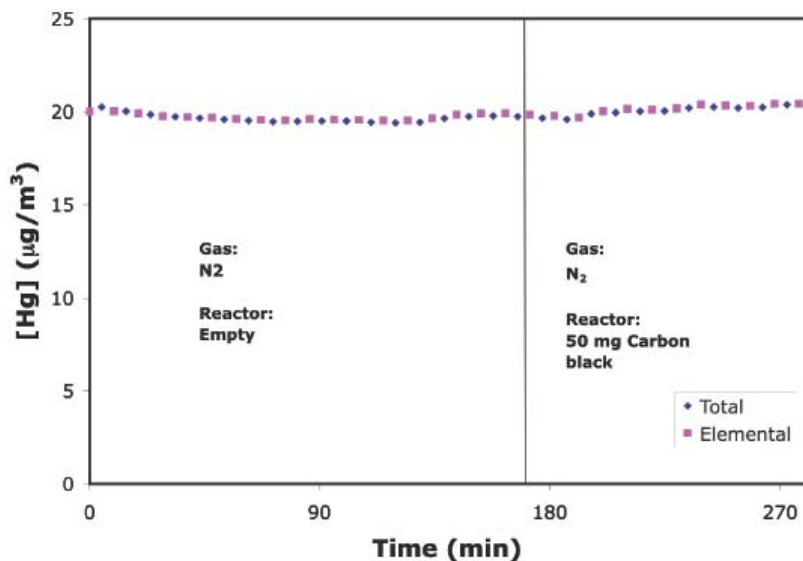


**Figure 26 Hg uptake by carbon black in  $N_2$  at 140 °C**

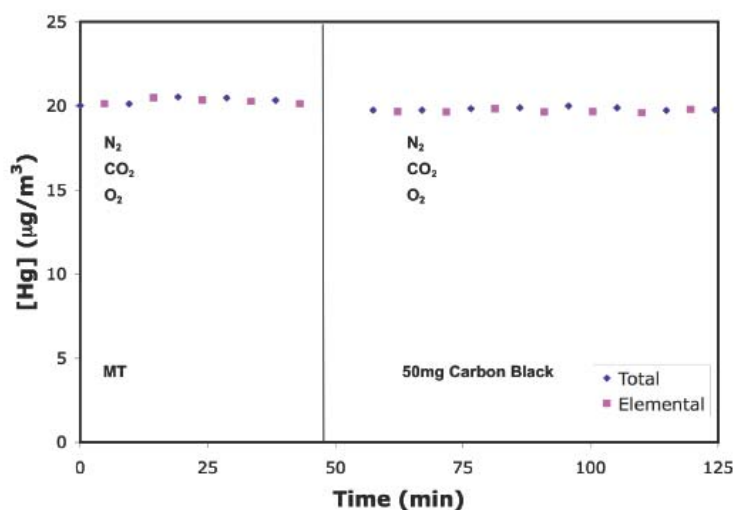
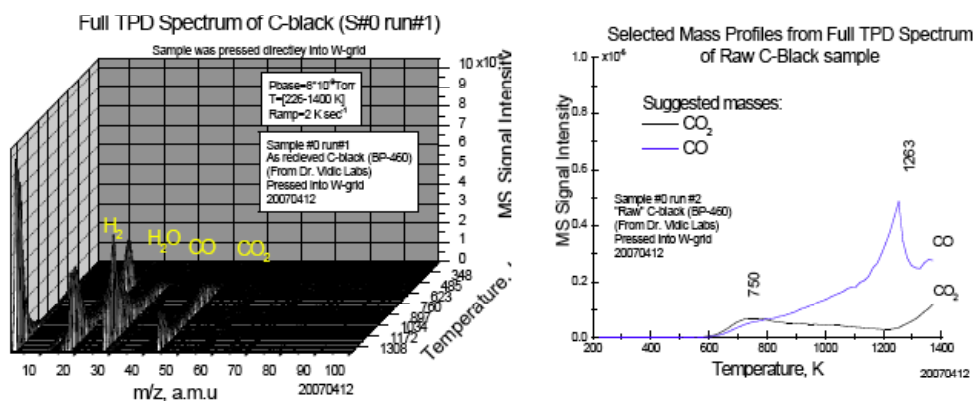


**Figure 27. Hg uptake by carbon black in  $N_2 + CO_2 + O_2$  at 140 °C**



Full TPD spectrum of as received C-black sample (#0). Heating of as received C-black sample is accompanied by desorption of CO and  $CO_2$  associated with the surface oxygen groups. Hydrogen desorbs as a product of cracking of surface C-H bonds.

**Figure 28. TPD analysis of as-received carbon black**

After the 100% breakthrough occurred, 1500ppm of  $SO_2$  was introduced to the influent stream. However, it did not promote mercury oxidation or mercury capture under both conditions (Figure 29 and 30). These results do not necessarily mean that  $SO_2$  will not inhibit mercury capture or oxidation, since no mercury was captured or oxidized

under these flue gas conditions. The effects of SO<sub>2</sub> will be discussed later regarding its interaction with HCl.

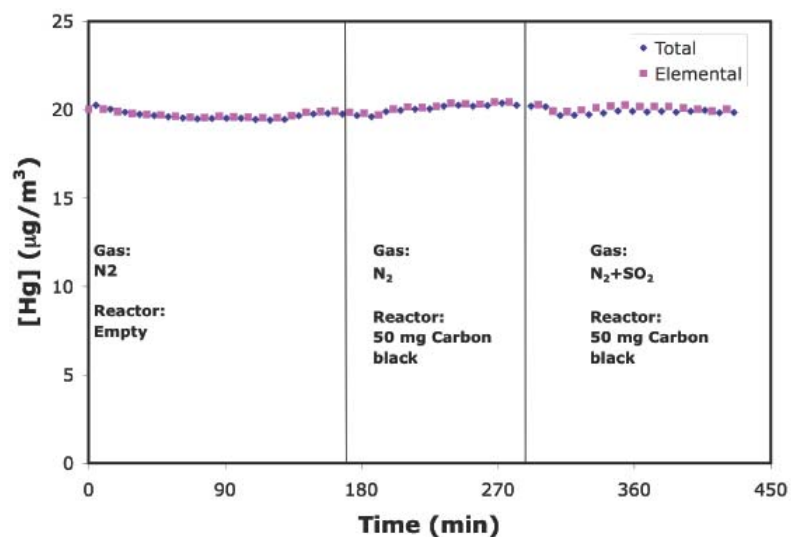


Figure 29. Effects of SO<sub>2</sub> on Hg uptake by carbon black in N<sub>2</sub> at 140 °C

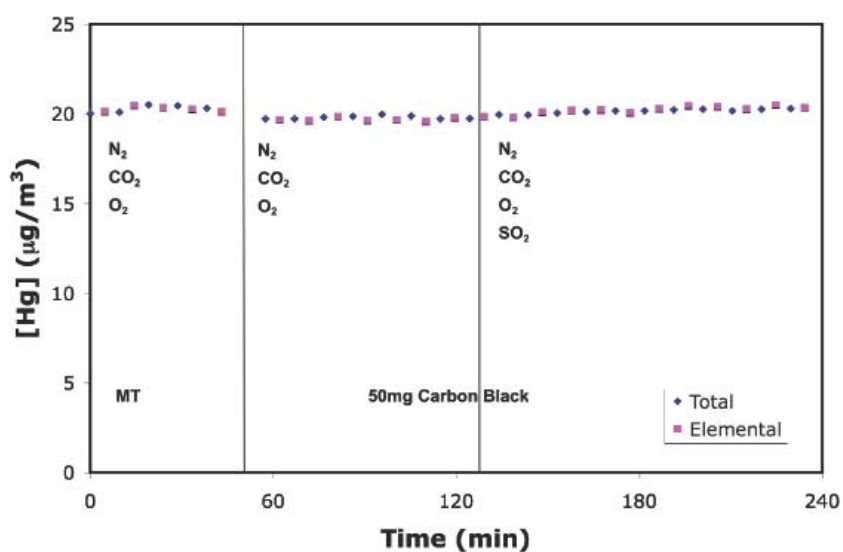
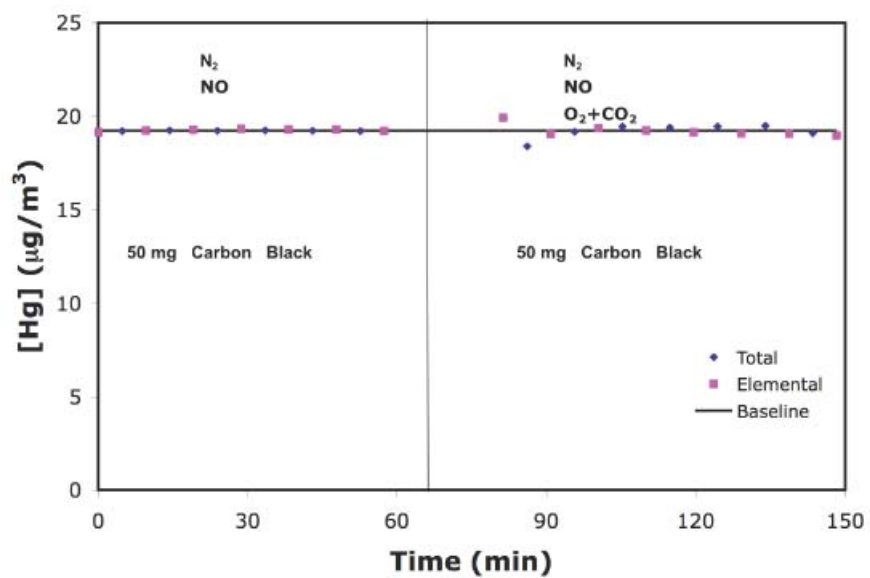


Figure 30. Effects of SO<sub>2</sub> on Hg uptake by carbon black in N<sub>2</sub> + CO<sub>2</sub> + O<sub>2</sub> at 140 °C

Similar to SO<sub>2</sub>, NO was found not to promote mercury oxidation or adsorption in either N<sub>2</sub> or N<sub>2</sub> + CO<sub>2</sub> + O<sub>2</sub>, as illustrated in Figure 31.



**Figure 31. Effects of NO on Hg uptake by carbon black at 140 °C**

Water vapor did not promote mercury adsorption or oxidation in the presence of  $\text{N}_2 + \text{CO}_2 + \text{O}_2$  (Figure 32).

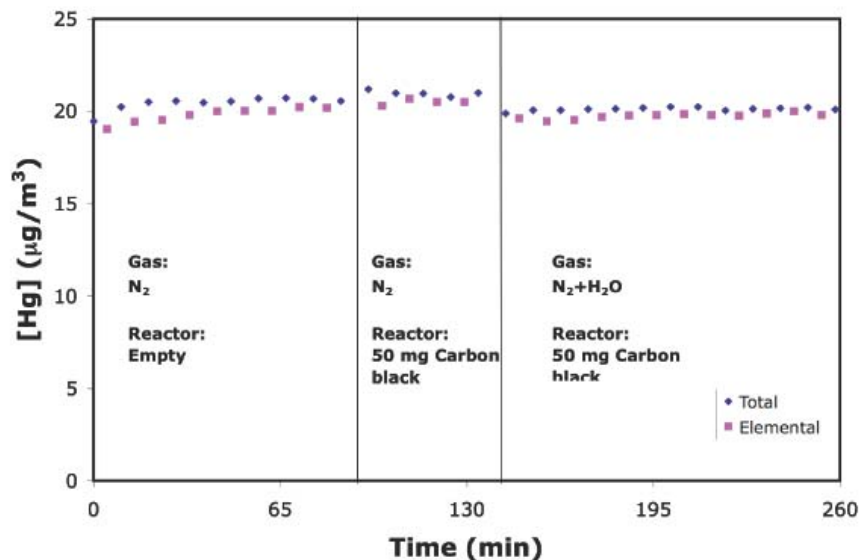


**Figure 32 Effects of  $\text{H}_2\text{O}$  on Hg uptake by carbon black in  $\text{N}_2 + \text{CO}_2 + \text{O}_2$  at 140 °C**

Previous experiments with fly ash or its components were all done without water vapor. One experiment with SH fly ash was done in a full flue gas with water vapor, as depicted in Figure 33.

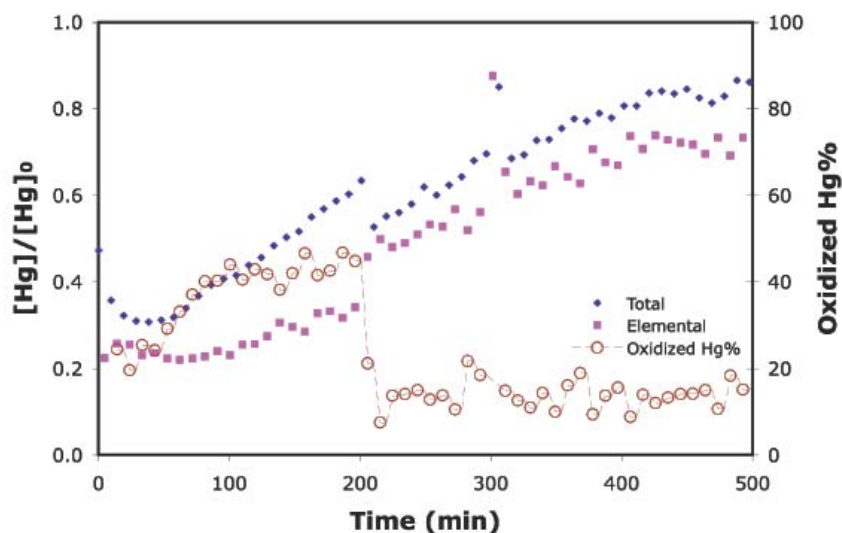


**Figure 33. Effects of H<sub>2</sub>O on Hg uptake by SH fly ash in flue gas at 140 °C**

A initial breakthrough of ~30% occurred immediately after the introduction of fly ash into the moisture containing flue gas, which was much higher than that (~5%) of the experiment with SH in flue gas without water vapor (Figure 14). However, 80% breakthrough occurred 1 hr later with water vapor than that without water vapor. As a result, a higher mercury adsorption onto fly ash was achieved with the presence of moisture (Table 12). It may be caused by changes on fly ash surfaces under long time exposure to water vapor containing flue gas. Water vapor seems to suppress mercury oxidation as shown from the comparison of oxidized mercury percentage in the effluent after 4-hr exposure (Table 12). However, under real power plant operation conditions, water vapor may inhibit mercury adsorption onto fly ash since the contact time between water vapor and fly ash particles would be 1 – 5 s, much shorter than that in the experiment in Figure 34.

**Table 12 Hg Uptake and Oxidation after Four-hour Exposure with SH Fly Ash in  
Flue Gas with and without Water Vapor**

| Flue gas                 | Mercury Load ( $\mu\text{g/g}$ ) | Oxidized Hg% |
|--------------------------|----------------------------------|--------------|
| With H <sub>2</sub> O    | 54.0                             | 14.26%       |
| Without H <sub>2</sub> O | 47.9                             | 22.89%       |

After NO<sub>2</sub> was introduced into N<sub>2</sub>, an immediate drop of both elemental and total mercury occurred (Figure 34). The elemental mercury in the effluent remained almost constant, while the total mercury slowly increased towards 100% breakthrough. Addition of CO<sub>2</sub> + O<sub>2</sub> did not have a significant impact on either oxidation or adsorption in the presence of NO<sub>2</sub> (Figure 35).

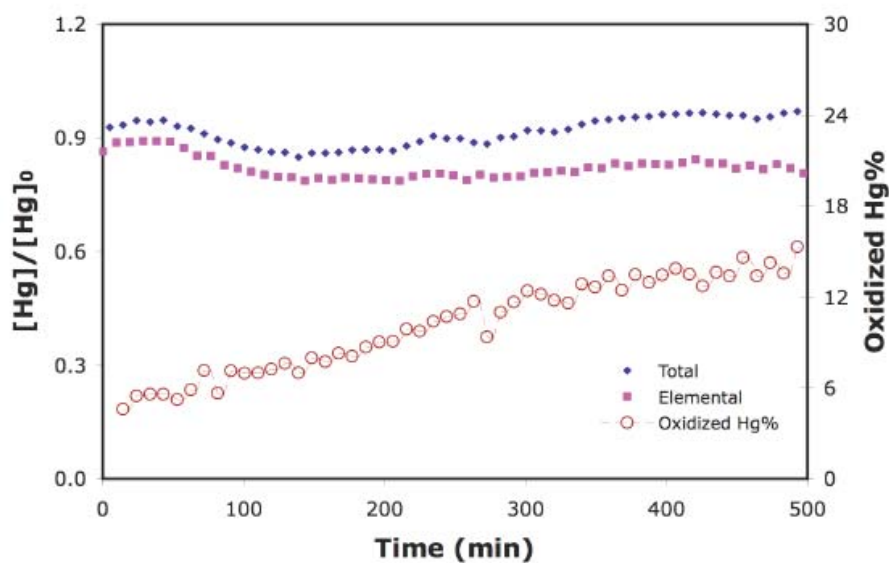


**Figure 34. Effects of NO<sub>2</sub> on Hg uptake by carbon black in N<sub>2</sub> at 140 °C**

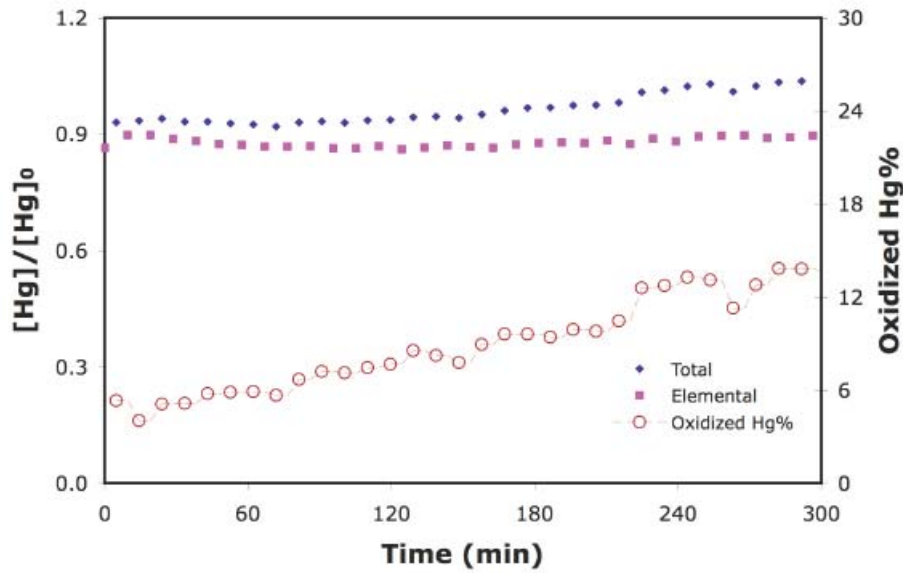


**Figure 35. Effects of NO<sub>2</sub> on Hg uptake by carbon black in N<sub>2</sub> + CO<sub>2</sub> + O<sub>2</sub> at 140 °C**

A 90% breakthrough occurred initially. After 100% breakthrough was achieved, oxidation still took place. It is generally believed that NO<sub>2</sub> could oxidize mercury and promote mercury capture onto carbon surface.<sup>6, 28, 57</sup> However, the exact mechanism is still unknown. Hg<sup>0</sup> is suggested to be oxidized by NO<sub>2</sub> and form Hg(NO<sub>3</sub>)<sub>2</sub> or HgO on the carbon surface, and part of NO<sub>2</sub> was reduced to NO by dismutation, as indicated in Reactions 18 and 19.<sup>57, 58</sup> NO is believed to transform into NO<sub>2</sub> in the presence of O<sub>2</sub> on the surface.<sup>49</sup> However, experiments summarized in Figure 32 revealed that with NO and O<sub>2</sub> in the gas phase, no mercury uptake or oxidation occurred. A possible mechanism for Hg oxidation by NO<sub>2</sub> could be oxidation only occurs between adsorbed Hg and gas-phase NO<sub>2</sub>, which is known as Eley-Rideal reaction (Reactions 20 and 21).<sup>27</sup>



For the case of mercury oxidation by NO<sub>2</sub>, A is Hg<sup>0</sup> and B is NO<sub>2</sub>.



HCl is an important parameter for mercury chemistry in coal-fired power plants. After HCl was introduced to N<sub>2</sub> gas flow, effluent Hg immediately dropped to around 70% of the inlet concentration (Figure 36). The behavior was similar to that observed for NO<sub>2</sub>. Elemental mercury in the effluent remained at 70% of the inlet level during the 12-hr test, while oxidized mercury slowly increased from 0 to 20% during that time. As HCl is not an oxidant, and the reaction between HCl and Hg is hindered by a very high energy barrier,<sup>7</sup> the surface must be responsible for electrons transfer.

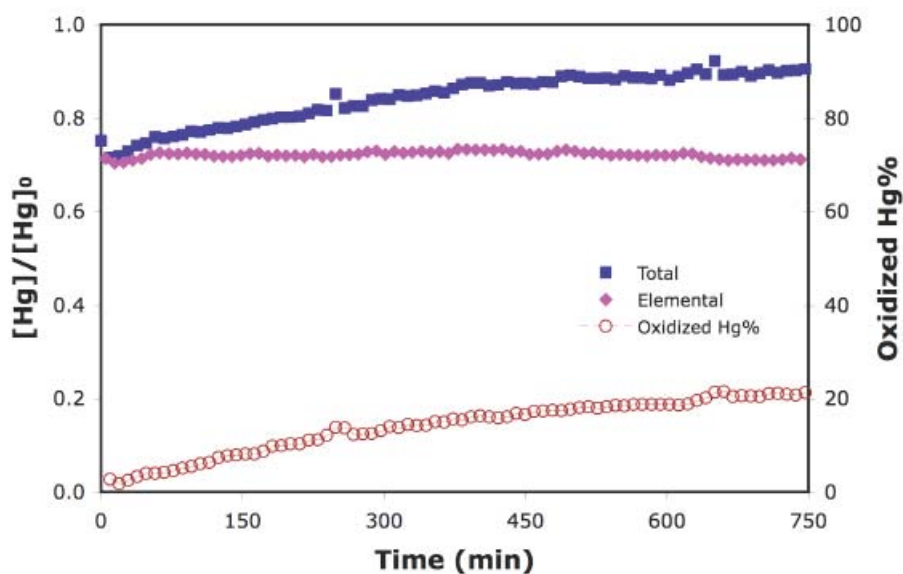


**Figure 36. Effects of HCl on Hg uptake by carbon black in N<sub>2</sub> at 140 °C**

A possible mechanism is that gas phase HCl impregnates the surface and creates Cl sites, which then react with Hg<sup>0</sup>.<sup>24</sup> However, neither TPD analyses nor XPS analyses of carbon black samples treated by N<sub>2</sub> + HCl (without Hg) revealed the existence of Cl on carbon surface (Table 11). It is possible that the binding energy between Cl and carbon

surface<sup>32</sup> is so low that Cl are removed under the ultra high vacuum conditions used in TPD and XPS analysis. However, previous studies<sup>29, 51, 56, 64</sup> have detected Cl on carbonaceous surfaces upon exposure to flue gas containing Hg. The difference could be due to the presence of Hg in these previous studies: Hg reacted with Cl containing species, and formed HgCl<sub>2</sub> being onto the surface resulted the Cl concentration increases in the samples.

Another hypothesis could be that Cl is catalytically generated by the interaction between HCl and the carbon surface,<sup>5</sup> while oxygen containing SFGs like oxygen functionalities may help to stable H atom attached on the surface.<sup>37</sup> In that case, Reaction 1:  $\text{Hg} + \text{Cl} \rightarrow \text{HgCl}$  could proceed. The resulted oxidized Hg species could be partially or completely adsorbed to surface, since the adsorption rate of HgCl<sub>2</sub> is higher than that of Hg<sup>0</sup>.<sup>46</sup>

The amount of elemental Hg remained at the same level during the experiment, which means the sum of adsorbed mercury and oxidized mercury remained constant too. Most likely, the surface has a constant capacity for mercury oxidation under the conditions of this experiment; some of the oxidized mercury is then adsorbed onto the carbon black, and as carbon black reaches its maximum capacity for oxidized mercury, 100% breakthrough occurs. If this is the case, the adsorption sites for elemental mercury would be different from oxidation sites and adsorption sites for oxidized mercury, and they were not present on the carbon black surface under the conditions in this experiment.

Addition of O<sub>2</sub> in the gas flow significantly improved mercury capture and oxidation (Figure 37). Elemental mercury in the effluent was decreasing in the first eight hours, which means that capacity of the surface for converting elemental mercury to

oxidized mercury and adsorbed Hg increased during that time. It is probably due to the changes in surface chemical properties under exposure to flue gas. However, as shown before (Figure 27), carbon black did not adsorb or oxidize any mercury in  $N_2 + CO_2 + O_2$ . Therefore, it is the interaction between  $O_2$  and HCl on the surface caused the promotion of mercury uptake and oxidation.

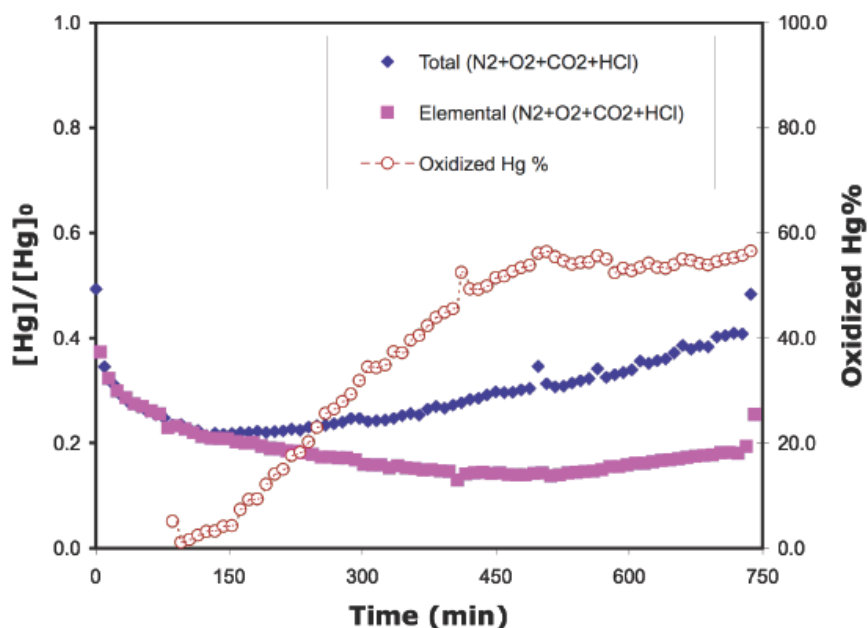
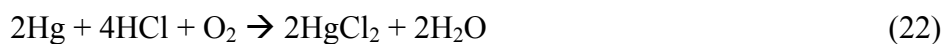


**Figure 37. Effects of HCl on Hg uptake by carbon black in  $N_2+CO_2+O_2$  at 140 °C**

A possible mechanism, the Deacon process, could be used to explain the effects of  $O_2$ . However, the Deacon process is generally catalyzed by metal compounds.<sup>16</sup> XPS analysis of the as-received carbon black revealed no metal elements existing on the surface (Table 11). The presence of mercury may drive the reaction forward without metal catalyst. The over all reaction could be,



In order to verify the effects of oxygen, 50 mg carbon black was exposed to 135ml/min  $O_2$  at 140 °C for 4 hrs. 1 L/min  $N_2$  with Hg was then sent to the treated

sample for 20 min to get rid of O<sub>2</sub> in the gas phase before introducing HCl. There was no oxidation or capture of mercury during the 20 min exposure to N<sub>2</sub> (Figure 38).

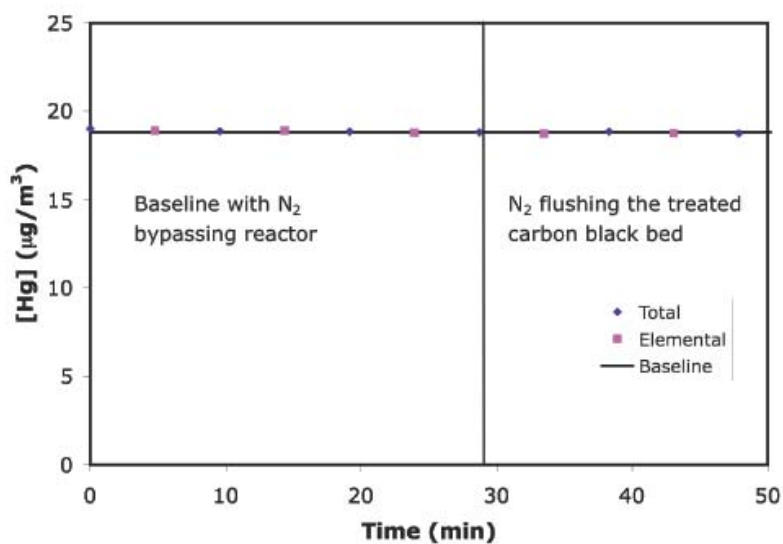
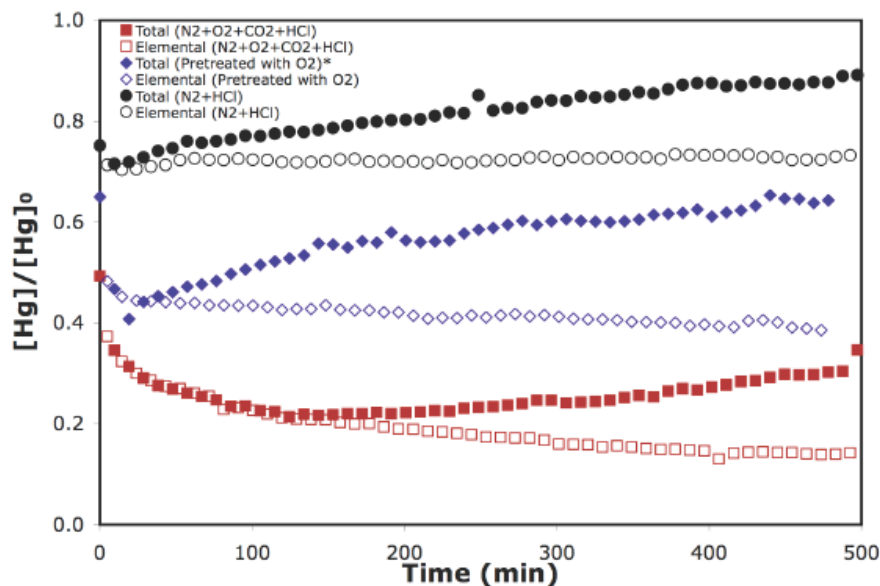


**Figure 38. Hg baseline in N<sub>2</sub> and its concentration in N<sub>2</sub> passed through O<sub>2</sub>-treated carbon black bed at 140 °C**

Introduction of HCl caused mercury capture instantly with the carbon black pretreated with O<sub>2</sub> (Figure 39, diamond symbols). Chemisorbed O<sub>2</sub> from the pretreatment accounts for the improvement in mercury capture and oxidation compared to the as-received carbon black (Figure 39, circle symbols). However, even with a four-hour exposure to O<sub>2</sub>, the carbon black sample still showed a higher initial mercury breakthrough than the one with O<sub>2</sub> in the gas stream (Figure 39, square symbols). This implied that O<sub>2</sub> in the gas phase more readily participates in the reaction than chemisorbed O<sub>2</sub> on carbon black. The net effect of oxygen functionalities can be similar to O<sub>2</sub> in gas phase, though the mechanisms involved are possibly much more complex.



\* Experiment with O<sub>2</sub> pretreated carbon black was then conducted in N<sub>2</sub> + HCl

**Figure 39. Effects of HCl on Hg uptake by carbon black in different gases at 140 °C**

Figure 40 depicts the effect of SO<sub>2</sub> in the influent flow of HCl + N<sub>2</sub> + CO<sub>2</sub> + O<sub>2</sub> on mercury capture and oxidation. SO<sub>2</sub> caused an appreciable decrease in mercury

capture and oxidized mercury percentage in the effluent. It most likely inhibited mercury capture and oxidation by competing for adsorption sites and electron acceptors. Both TPD and XPS analyses (Table 11) indicated the adsorption of S on the surface, which at least supported the idea of competition for adsorption sites.<sup>54</sup> Previous experimental findings showed that SO<sub>2</sub> is generally being adsorbed on the carbon surface in S(VI) form,<sup>29, 55, 56</sup> which means it would compete with Hg for electron acceptors in order to be oxidized. SO<sub>2</sub> may inhibit the adsorption of O<sub>2</sub> onto the surface, and then result in a decrease in mercury oxidation.

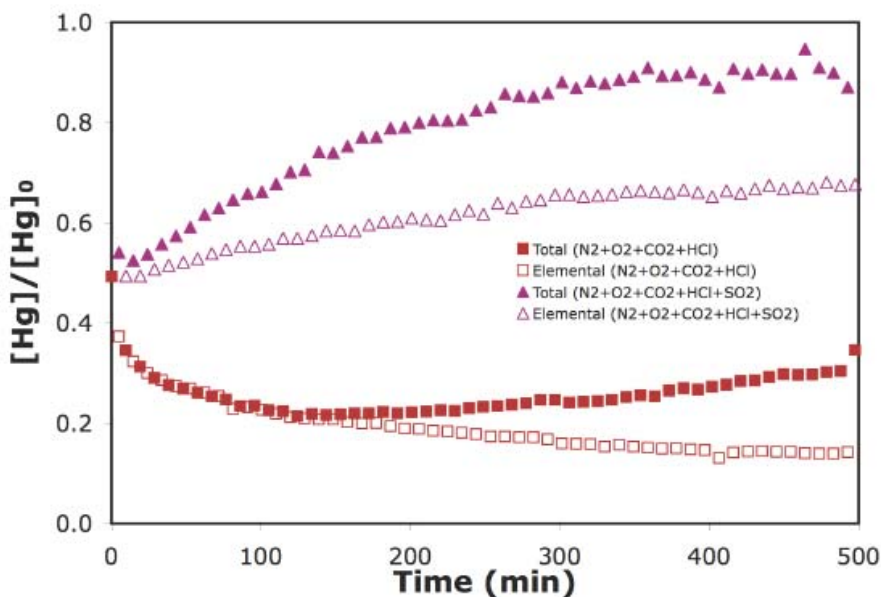


**Figure 40. Effects of SO<sub>2</sub> on Hg uptake by carbon black in HCl + N<sub>2</sub> + CO<sub>2</sub> + O<sub>2</sub> at 140 °C**

From experiments with carbon black in different gas combination, it could be concluded that carbon black does not adsorb or oxidize mercury in N<sub>2</sub> even in the presence of O<sub>2</sub>. NO<sub>2</sub> could promote mercury oxidation and adsorption without HCl and O<sub>2</sub>. NO, SO<sub>2</sub> or H<sub>2</sub>O does not promote mercury oxidation or adsorption by itself. H<sub>2</sub>O

seems to inhibit mercury adsorption upon its introduction into gas stream. However, over time its effect on mercury adsorption diminished, though it suppressed mercury oxidation. HCl has profound effects on mercury adsorption and capture, especially when oxygen is present. SO<sub>2</sub> tends to diminish the effects of HCl by occupying the binding sites and competing for electron acceptors with mercury. It can also be concluded that the flue gas composition and the interaction between flue gas and the surfaces are more important than the fly ash composition, though the presence of fly ash samples play a predominant role in mercury oxidation.<sup>28</sup>

## 5.0 SUMMARY AND CONCLUSIONS

Increases in LOI value (unburned carbon) of fly ash samples resulted in improvements in mercury capture and oxidation. Mercury capture and oxidation were proportional to surface area for different samples. Particle size exhibited similar effects to surface area. The impacts of surface area and particle size were similar to those of LOI, which could be explained by the facts that unburned carbon in fly ash has a relatively high surface area than other fractions, and it tends to be enriched in coarser fractions compared with other fractions in the samples.<sup>41, 48</sup>

Tests with single fly ash components indicated that  $\text{SiO}_2$ ,  $\text{Al}_2\text{O}_3$ ,  $\text{MgO}$ ,  $\text{CaO}$ , and  $\text{TiO}_2$  had little effect on promoting mercury oxidation or adsorption.  $\text{Fe}_2\text{O}_3$  and carbon black promoted both mercury oxidation and adsorption. However, carbon was considered as the most important component because of its higher content in different samples compared with iron.

The interaction between flue gas components and surfaces is found to have significant effects on mercury transformation.  $\text{NO}$ ,  $\text{O}_2$ ,  $\text{H}_2\text{O}$ , and  $\text{SO}_2$  did not promote mercury oxidation or capture on carbon black by themselves.  $\text{NO}_2$  can help oxidize and capture mercury on carbon black with or without  $\text{O}_2$ .  $\text{HCl}$  showed the most profound effects on mercury oxidation and capture.  $\text{O}_2$  plays an important role when combined with  $\text{HCl}$ , where the Deacon process could be involved.  $\text{SO}_2$  inhibited mercury oxidation and



capture probably by competing for electron acceptors with mercury and occupying the adsorption sites on the surface.

## BIBLIOGRAPHY

1. U.S. Environmental Protection Agency Mercury Basic Information. <http://www.epa.gov/mercury/about.htm> (May 14th)
2. U.S. Environmental Protection Agency *Mercury Study Report to Congress Volume I: Executive Summary*; Office of Air Quality Planning and Standards and Office of Research and Development: Dec., 1997.
3. Galbreath, K. C.; Zygarlicke, C. J., Mercury transformations in coal combustion flue gas. *Fuel Processing Technology* **2000**, 65, 289-310.
4. Pavlish, J. H.; Sondreal, E. A.; Mann, M. D.; Olson, E. S.; Galbreath, K. C.; Laudal, D. L.; Benson, S. A., State review of mercury control options for coal-fired power plants. *Fuel Processing Technology* **2003**, 82, (2-3), 89-165.
5. Sliger, R. N.; Kramlich, J. C.; Marinov, N. M., Towards the development of a chemical kinetic model for the homogeneous oxidation of mercury by chlorine species. *Fuel Processing Technology* **2000**, 65-66, 423-438.
6. Hall, B.; Schager, P.; Lindqvist, O., Chemical reactions of mercury in combustion flue gases. *Water, Air, & Soil Pollution* **1991**, 56, (1), 3-14.
7. Senior, C. L.; Sarofim, A. F.; Zeng, T. F.; Helble, J. J.; Mamani-Paco, R., Gas-phase transformations of mercury in coal-fired power plants. *Fuel Processing Technology* **2000**, 63, (2-3), 197-213.
8. Edwards, J. R.; Srivastava, R. K.; Kilgroe, J. D., A Study of Gas-Phase Mercury Speciation Using Detailed Chemical Kinetics. *Journal of the Air & Waste Management Association* **2001**, 51, (6), 869-877.
9. Niksa, S.; Helble, J. J.; Fujiwara, N., Kinetic Modeling of Homogeneous Mercury Oxidation: the importance of NO and H<sub>2</sub>O in predicting oxidation in coal-derived systems. *Environ. Sci. Technol* **2001**, 35, (18), 3701-3706.
10. Xu, M. H.; Qiao, Y.; Zheng, C. G.; Li, L. C.; Liu, J., Modeling of homogeneous mercury speciation using detailed chemical kinetics. *Combustion and Flame* **2003**, 132, (1-2), 208-218.

11. Agarwal, H.; Stenger, H. G.; Wu, S.; Fan, Z., Effects of H<sub>2</sub>O, SO<sub>2</sub>, and NO on homogeneous Hg oxidation by Cl<sub>2</sub>. *Energy & Fuels* **2006**, 20, (3), 1068-1075.
12. Zhao, Y. X.; Mann, M. D.; Olson, E. S.; Pavlish, J. H.; Dunham, G. E., Effects of sulfur dioxide and nitric oxide on mercury oxidation and reduction under homogeneous conditions. *Journal Of The Air & Waste Management Association* **2006**, 56, (5), 628-635.
13. Agarwal, H.; Romero, C. E.; Stenger, H. G., Comparing and interpreting laboratory results of Hg oxidation by a chlorine species. *Fuel Processing Technology* **2007**, 88, (7), 723-730.
14. Agarwal, H.; Stenger, H. G., Development of a predictive kinetic model for homogeneous Hg oxidation data. *Mathematical and Computer Modelling* **2007**, 45, (1-2), 109-125.
15. Laudal, D. L.; Brown, T. D.; Nott, B. R., Effects of flue gas constituents on mercury speciation. *Fuel Processing Technology* **2000**, 65-66, 157-165.
16. Pan, H. Y.; Minet, R. G.; Benson, S. W.; Tsotsis, T. T., Process for Converting Hydrogen Chloride to Chlorine. *Ind. Eng. Chem. Res.* **1994**, 33, (12), 2996-3003.
17. Hall, B.; Schager, P.; Weesmaa, J., The homogeneous gas phase reaction of mercury with oxygen, and the corresponding heterogeneous reactions in the presence of activated carbon and fly ash. *Chemosphere* **1995**, 30, (4), 611-627.
18. Mamani-Paco, R. M.; Helble, J. J., Bench Scale Examination of Mercury Oxidation under Non-Isothermal Conditions. *93rd Annual Meeting, Air&Waste Management Association, Salt Lake City, Utah* **2000**.
19. Thomas J. Feeley, I.; Murphy, J.; Hoffmann, J.; Renninger, S. A. *A review of DOE/NETL's mercury control technology R&D program for coal-fired power plant*; April, 2003.
20. Yudovich, Y. E.; Ketris, M. P., Mercury in coal: a review. Part 2. Coal use and environmental problems. *International journal of coal geology* **2005**, 62, (3), 135-165.
21. Kilgroe, J. D.; Sedman, C. B.; Srivastava, R. K.; Ryan, J. V.; Lee, C. W.; Thorneloe, S. A. *Control of Mercury Emissions from Coal-Fired Electric Utility Boilers: Interim Report*; US Environmental Protection Agency, Office of Research and Development, National Risk Management Laboratory, Air Pollution Prevention and Control Division: Research Triangle Park, March, 2002.
22. Kellie, S.; Cao, Y.; Duan, Y.; Li, L.; Chu, P.; Mehta, A.; Carty, R.; Riley, J. T.; Pan, W. P., Factors Affecting Mercury Speciation in a 100-MW Coal-Fired Boiler with Low-NO<sub>x</sub> Burners. *Energy Fuels* **2005**, 19, (3), 800-806.

23. Fujiwara, N.; Fujita, Y.; Tomura, K.; Moritomi, H.; Tuji, T.; Takasu, S.; Niksa, S., Mercury transformations in the exhausts from lab-scale coal flames. *Fuel* **2002**, 81, (16), 2045-2052.
24. Huggins, F. E.; Yap, N.; Huffman, G. P.; Senior, C. L., XAFS characterization of mercury captured from combustion gases on sorbents at low temperatures. *Fuel Processing Technology* **2003**, 82, (2-3), 167-196.
25. Lopez-Anton, M. A.; Diaz-Somoano, M.; Abad-Valle, P.; Martinez-Tarazona, M. R., Mercury and selenium retention in fly ashes: Influence of unburned particle content. *Fuel* **2007**, doi: 10.1016/j.fuel.2007.03.031.
26. Dunham, G. E.; DeWall, R. A.; Senior, C. L., Fixed-bed studies of the interactions between mercury and coal combustion fly ash. *Fuel Processing Technology* **2003**, 82, (2-3), 197-213.
27. Presto, A. A.; Granite, E. J., Survey of Catalysts for Oxidation of Mercury in Flue Gas. *Environ. Sci. Technol.* **2006**, 40, (18), 5601-5609.
28. Norton, G. A.; Yang, H.; Brown, R. C.; Laudal, D. L.; Dunham, G. E.; Erjavec, J., Heterogeneous oxidation of mercury in simulated post combustion conditions. *Fuel* **2003**, 82, (2), 107-116.
29. Huggins, F. E.; Huffman, G. P.; Dunham, G. E.; Senior, C. L., XAFS examination of mercury sorption on three activated carbons. *Energy & Fuels* **1999**, 13, (1), 114-121.
30. Hutson, N. D.; Attwood, B. C.; Scheckel, K. G., XAS and XPS Characterization of Mercury Binding on Brominated Activated Carbon. *Environ. Sci. Technol* **2007**, 41, (5), 1747-1752.
31. Ghorishi, S. B.; Keeney, R. M.; Serre, S. D.; Gullett, B. K.; Jozewicz, W. S., Development of a Cl-impregnated activated carbon for entrained-flow capture of elemental mercury. *Environmental Science & Technology* **2002**, 36, (20), 4454-4459.
32. Podak, B.; Brunetti, M.; Lewis, A.; Wilcox, J., Mercury binding on activated carbon. *Environmental Progress* **2006**, 25, (4), 319-326.
33. Vidic, R. D.; Siler, D. P., Vapor-phase elemental mercury adsorption by activated carbon impregnated with chloride and chelating agents. *Carbon* **2001**, 39, (1), 3-14.
34. Lee, S. J.; Seo, Y.-C.; Jurng, J.; Lee, T. G., Removal of gas-phase elemental mercury by iodine- and chlorine-impregnated activated carbons. *Atmospheric Environment* **2004**, 38, (29), 4887-4893.
35. Kwon, S.; Borguet, E.; Vidic, R. D., Impact of Surface Heterogeneity on Mercury Uptake by Carbonaceous Sorbents under UHV and Atmospheric Pressure. *Environmental Science & Technology* **2002**, 36, (19), 4162-4169.

36. Li, Y. H.; Lee, C. W.; Gullett, B. K., Importance of activated carbon's oxygen surface functional groups on elemental mercury adsorption\*. *Fuel* **2003**, 82, (4), 451-457.
37. Perez-Cadenas, A. F.; Maldonado-Hodar, F. J.; Moreno-Castilla, C., On the nature of surface acid sites of chlorinated activated carbons. *Carbon* **2003**, 41, (3), 473-478.
38. Serre, S. D.; Silcox, G. D., Adsorption of elemental mercury on the residual carbon in coal fly ash. *Industrial & Engineering Chemistry Research* **2000**, 39, (6), 1723-1730.
39. Ghorishi, B.; Gullett, B. K., Sorption of mercury species by activated carbons and calcium-based sorbents: effect of temperature, mercury concentration and acid gases. *Waste Management & Research* **1998**, 16, 582-593.
40. Thorwarth, H.; Stack-Lara, V.; Unterberger, S.; Scheffknecht, G. In *The Influence of Fly Ash Constituents on Mercury Speciation, the Air Quality V: Mercury, Trace Elements, SO<sub>3</sub>, and Particulate Matter Conference*, Arlington, VA, Sept. 19-21, 2005; Arlington, VA, 2005.
41. Hwang, J. Y.; Sun, X.; Li, Z., Unburned Carbon from Fly Ash for Mercury Adsorption: I. Separation and Characterization of Unburned Carbon. *Journal of Minerals & Materials Characterization & Engineering* **2002**, 1, (1), 39-60.
42. Senior, C. L.; Johnson, S. A., Impact of Carbon-in-Ash on Mercury Removal across Particulate Control Devices in Coal-Fired Power Plants. *Energy Fuels* **2005**, 19, (3), 859-863.
43. Maroto-Valer, M. M.; Zhang, Y. Z.; Granite, E. J.; Tang, Z.; Pennline, H. W., Effect of porous structure and surface functionality on the mercury capacity of a fly ash carbon and its activated sample. *Fuel* **2005**, 84, (1), 105-108.
44. Hassett, D. J.; Eylands, K. E., Mercury capture on coal combustion fly ash. *Fuel* **1999**, 78, (2), 243-248.
45. Hower, J. C.; Maroto-Valer, M. M.; Taulbee, D. N.; Sakulpitakphon, T., Mercury capture by distinct fly ash carbon forms. *Energy & Fuels* **2000**, 14, (1), 224-226.
46. Carey, T. R.; Oliver W. Hargrove, J.; Richardson, C. F.; Chang, R.; Meserole, F. B., Factors Affecting Mercury Control in Utility Flue Gas Using Activated Carbon. *Journal Of The Air & Waste Management Association* **1998**, 48, 1166-1174.
47. Baltrus, J. P.; Wells, A. W.; Fauth, D. J.; Diehl, J. R.; White, C. M., Characterization of Carbon Concentrates from Coal-Combustion Fly Ash. *Energy Fuels* **2001**, 15, (2), 455-462.

48. Suraez-Ruiz, I.; Parra, J. B., Relationship between Textural Properties, Fly Ash Carbons, and Hg Capture in Fly Ashes Derived from the Combustion of Anthracitic Pulverized Feed Blends. *Energy Fuels* **2007**.
49. Rubel, A.; Andrews, R.; Gonzalez, R.; Groppo, J.; Robl, T., Adsorption of Hg and NOX on coal by-products. *Fuel* **2005**, 84, (7-8), 911-916.
50. Ghorishi, S. B.; Lee, C. W.; Jozewicz, W. S.; Kilgroe, J. D., Effects of fly ash transition metal content and flue gas HCl/SO<sub>2</sub> ratio on mercury speciation in waste combustion. *Environmental Engineering Science* **2005**, 22, (2), 221-231.
51. Galbreath, K. C.; Zygarlicke, C. J.; Tibbetts, J. E.; Schulz, R. L.; Dunham, G. E., Effects of NO<sub>x</sub>,  $\alpha$ -Fe<sub>2</sub>O<sub>3</sub>,  $\gamma$ -Fe<sub>2</sub>O<sub>3</sub>, and HCl on mercury transformations in a 7-kW coal combustion system. *Fuel Processing Technology* **2004**, 86, (4), 429-448.
52. Zeng, H.; Jin, F.; Guo, J., Removal of elemental mercury from coal combustion flue gas by chloride-impregnated activated carbon. *Fuel* **2004**, 83, (1), 143-146.
53. Miller, S. J.; Dunham, G. E.; Olson, E. S.; Brown, T. D., Flue gas effects on a carbon-based mercury sorbent. *Fuel Processing Technology* **2000**, 65-66, 343-363.
54. Laumb, J. D.; Benson, S. A.; Olson, E. A., X-ray photoelectron spectroscopy analysis of mercury sorbent surface chemistry. *Fuel Processing Technology* **2004**, 85, (6-7), 577-585.
55. Davini, P., Flue gas desulphurization by activated carbon fibers obtained from polyacrylonitrile by-product. *Carbon* **2003**, 41, (2), 277-284.
56. Morimoto, T.; Wu, S.; Azhar Uddin, M.; Sasaoka, E., Characteristics of the mercury vapor removal from coal combustion flue gas by activated carbon using H<sub>2</sub>S. *Fuel* **2005**, 84, (14-15), 1968-1974.
57. Galbreath, K. C.; Zygarlicke, C. J., Mercury Speciation in Coal Combustion and Gasification Flue Gases. *Environ. Sci. Technol.* **1996**, 30, (8), 2421-2426.
58. Olson, E. S.; Dunham, G. E.; Sharma, R. K.; Miller, S. J., Mechanisms of mercury capture and breakthrough on activated carbon sorbents. In *American Chemical Society National Meeting*, Washington DC, 2000; pp 886-889.
59. Li, Y. H.; Lee, C. W.; Gullett, B. K., The effect of activated carbon surface moisture on low temperature mercury adsorption. *Carbon* **2002**, 40, (1), 65-72.
60. Senior, C.; Bustard, C. J.; Durham, M.; Baldrey, K.; Michaud, D., Characterization of fly ash from full-scale demonstration of sorbent injection for mercury control on coal-fired power plants. *Fuel Processing Technology* **2004**, 85, (6-7), 601-612.
61. U.S. Environmental Protection Agency *Control of Mercury Emissions from Coal Fired Electric Utility Boilers: An Update*; Research Triangle Park, February 18, 2005.

62. Lei, C.; Yufeng, D.; Yuqun, Z.; Ligu, Y.; Liang, Z.; Xianghua, Y.; Qiang, Y.; Yiman, J.; Xuchang, X., Mercury transformation across particulate control devices in six power plants of China: The co-effect of chlorine and ash composition. *Fuel* **2007**, 86, (4), 603-610.
63. Presto, A. A.; Granite, E. J.; Karash, A.; Hargis, R. A.; O'Dowd, W. J.; Pennline, H. W., A kinetic approach to the catalytic oxidation of mercury in flue gas. *Energy & Fuels* **2006**, 20, (5), 1941-1945.
64. Olson, E. S.; Crocker, C. R.; Benson, S. A.; Pavlish, J. H.; Holmes, M. J., Surface compositions of carbon sorbents exposed to simulated low-rank coal flue gases. *Journal of the Air & Waste Management Association* **2005**, 55, (6), 747-754.